

Review

Not peer-reviewed version

---

# Surface Treatment of Biochar—Methods, Surface Analysis and Potential Applications: A Comprehensive Review

---

[Marlena Gęca](#) , [Ahmed M. Khalil](#) , [Arvind K. Bhakta](#) , [Youssef Snoussi](#) , [Piotr Nowicki](#) , [Małgorzata Wiśniewska](#) , [Mohamed M. Chehimi](#) \*

Posted Date: 20 March 2023

doi: 10.20944/preprints202303.0353.v1

Keywords: biomass conversion; thermochemical treatment; surface chemical modification; coupling agents; biochar implementation



Preprints.org is a free multidiscipline platform providing preprint service that is dedicated to making early versions of research outputs permanently available and citable. Preprints posted at Preprints.org appear in Web of Science, Crossref, Google Scholar, Scilit, Europe PMC.

Copyright: This is an open access article distributed under the Creative Commons Attribution License which permits unrestricted use, distribution, and reproduction in any medium, provided the original work is properly cited.

## Article

# Surface Treatment of Biochar—Methods, Surface Analysis and Potential Applications: A Comprehensive Review

Marlena Gęca <sup>1</sup>, Ahmed M. Khalil <sup>2,3,\*</sup>, Arvind K. Bhakta <sup>3</sup>, Youssef Snoussi <sup>3</sup>, Piotr Nowicki <sup>4</sup>, Małgorzata Wiśniewska <sup>1,\*</sup> and Mohamed M. Chehimi <sup>3,\*</sup>

<sup>1</sup> Department of Radiochemistry and Environmental Chemistry, Institute of Chemical Sciences, Faculty of Chemistry, Maria Curie-Skłodowska University in Lublin, M. Curie-Skłodowska Sq. 3, 20-031 Lublin, Poland

<sup>2</sup> Photochemistry Department, National Research Centre, Dokki, 12622 Giza, Egypt

<sup>3</sup> Université de Paris, CNRS, ITODYS (UMR 7086), 75013 Paris, France

<sup>4</sup> Department of Applied Chemistry, Faculty of Chemistry, Adam Mickiewicz University in Poznań, Uniwersytetu Poznańskiego 8, 61-614 Poznań, Poland

\* Correspondence: akhalil75@yahoo.com (A.M.K.); malgorzata.wisniewska@mail.umcs.pl (M.W.); mohamed.chehimi@cnrs.fr (M.M.C.)

**Abstract:** In the recent years, biochar has emerged as a remarkable biosourced material for addressing global environmental, agricultural, biomedical, and energy challenges. However, the performances of biochar rest in part on finely tuning its surface chemical properties, intended to obtain specific functionalities. In this review, we tackle surface treatment of biochar with silane and other coupling agents such as diazonium salts, titanates, ionic/non-ionic surfactants, as well as nitrogen-containing (macro)molecules. We summarize the recent progress achieved mostly in the last five years, and correlate the nature and extent of functionalization to eye catchy end applications of the surface engineered biochar.

**Keywords:** Biomass conversion; thermochemical treatment; surface chemical modification; coupling agents; biochar implementation

## 1. Introduction and Scope of the Review

It is without any doubt that biochar is a very hot topic, due to its central position, at the cross-roads of materials science, materials and surface chemistry, surface science, catalysis and organic reactions. Biochar is at the heart of sustainable development, and concerns biomass and waste valorization, and utilization for depollution and soil amendment. Such an infatuation for biochar is motivated by the availability of numerous varieties of biomasses and wastes worldwide, and the need for valorization and/or transformation into functional materials. This resulted in sky rocketing number of publications, exceeding 5500 since 2021.

The most important applications of biochar concern soil amendment and agriculture [1–3], but recently much has been achieved in the design of biochar-supported nanocatalysts for water treatment consisting in total mineralization of organic pollutants such as dyes and drugs [4,5]. Other applications concern the use of biochar as fillers in composite materials [6–8], electrode materials [9,10] and for the developments of novel engineered biochar for the treatment of neglected tropical diseases (NTDs) [11,12], to name but these applications.

Whilst biochar can be employed as freshly obtained by thermochemical conversion of the biomass, it nevertheless requires particular surface treatment in order to impart it with new functionalities. In this mini-review, the focus is on coupling agents rather than the traditional acid or alkali treatment and other activations strategies; the latter could easily be found in several review papers. We have shortlisted some of them in Table 1.

**Table 1.** Shortlisted, relevant reviews tackling applications of surface engineered biochar.

Running title	Review main topic	Year review published	References
Biochar for catalytic biorefinery and environmental processes	The article summarizes the knowledge on the production of biochar, its classical activation with aggressive compounds and its use to expediate biorefinery operations and degradation of environmental pollutants	2019	[13]
Chemically modified carbonaceous adsorbents for CO <sub>2</sub> capture	The review discusses activation, surface amination or carboxylation, and doping of various carbon allotropes, including biochar, for extensive capture of CO <sub>2</sub> .	2021	[14]
Biochar as a support for nanocatalysts and other reagents	The review paper summarizes the knowledge on the use of biochar-supported nanocatalyst, and discusses the mode of coordination of the catalyst nanoparticles by the biochar.	2021	[15]
Phosphorus adsorption by functionalized biochar	Inefficient crop fertilization induces water pollution by phosphorus. The review discusses biomass pre-treatment as well as post-modification of biochar to obtain efficient phosphorus porous adsorbents	2022	[16]
Surface modification of biochar for dye removal	The review discusses several strategies of obtaining functional biochar for the removal of dyes from water.	2022	[17]
Biochar for the removal of contaminants from industrial wastewaters	The paper reviews methods for obtaining pristine and engineered biochar for the efficient removal of numerous contaminants from industrial wastewaters.	2022	[18]
Biochar as a reinforcing bio-based filler in rubber composites.	This article is focussed on the key properties of highly reinforcing fillers such as particle size, structure, and surface activity are discussed. The review essentially covers silane modification of biochar.	2023	[7]

The shortlisted reviews concerned various carbon allotrope surface modification [14], classical activation methods [13] that rest on acid or alkali treatment of biochar, activation with metal chlorides, post pyrolysis under steam to name but a few. However, despite the numerous advances in biochar production, post-modification and applications, only a few reviews covered surface modification, for example the surface treatment of biochar particles with silanes for the design of high performance composites (see Table 1). Coverage of the chemical modification of biochar surface with a large series of well-known coupling agents such as silanes, diazonium salts, aminated compounds, surfactants and macromolecules is lacking despite its interest in several domains, i.e., organic chemistry, polymer science and technology, environmental remediation, and sustainable energy. This is what has motivated this review article.

**2. Biochar Surface Treatment Pathways**

*2.1. General Aspects*

Figure 1 schematically illustrates shortlisted pathways for chemical modification of biochar surface. The literature survey using Google Scholar and the Web of Science indicated that the most employed compounds are silane coupling agents, ionic or non-ionic surfactants, and aryl diazonium salts. For catalytic purposes, titanates have also been proposed. Silanes require hydroxylated surfaces and thus are applicable to biochar as most of biochar materials are prepared by thermochemical conversion at 300-500 °C, a range of temperature that ensures the presence of reactive functional groups such as OH and C=O [17]. Such groups can also be obtained by post acidic treatment [17,19]. Concerning diazonium salts, most carbon allotropes react with these modern surface modifiers to provide C-C bonds and ester linkages [20]. As far as surfactants are concerned, anionic and cationic surfactants interact with biochar via complete different mechanisms (biochar-hydrophobic tail, or biochar-hydrophilic head) [21]. Non-ionic surfactants have completely different behaviour, and rather interact with biochar via oxygen atoms or OH groups (see Section 2.4). Titanate are able to

form  $\text{TiO}_2$  nanoparticles, in situ, at the surface of biochar and thus important for providing photocatalytic composites [22]. Other emerging coupling agents are polyethyleneimine (PEI) [23].

In this review, we concentrate on coupling agents that react/interact chemically with biochar, via covalent linkages or through strong electrostatic interactions, hydrogen bonds or hydrophobic interactions. Other strategies consisting in direct immobilization of nanocatalysts on biochar obtained by pyrolysis of biomass impregnated with metal salt precursor will be briefly summarized at the end of the review.

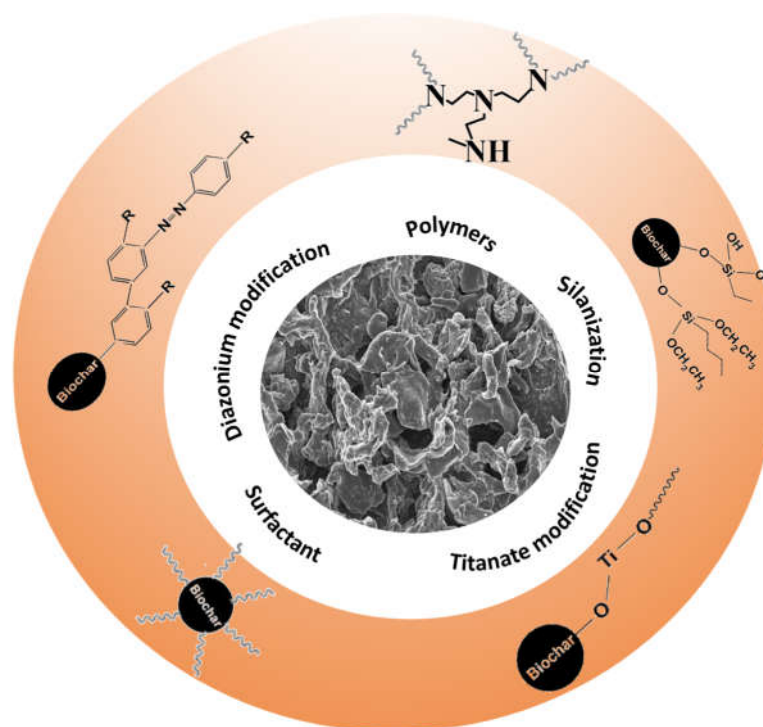


**Figure 1.** Schematic illustration of biochar surface treatment with popular coupling agents.

## 2.2. Surface Functionalization with Silane Coupling Agents

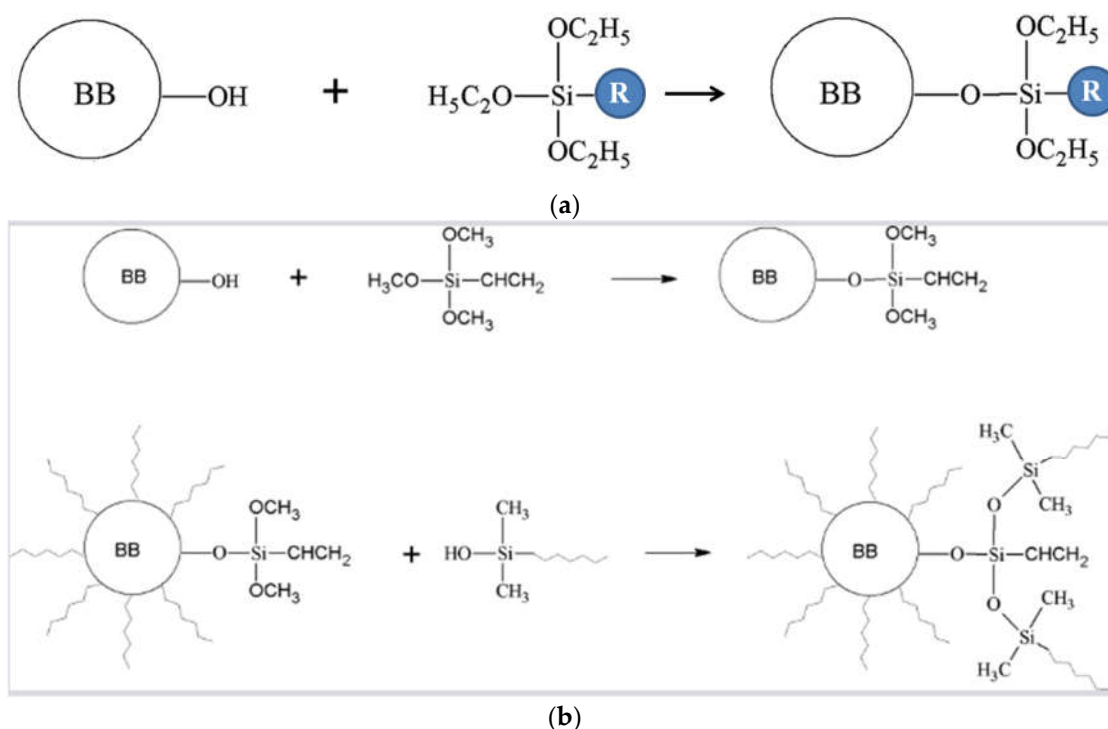
Silanization is the process of modification of surfaces by incorporating organofunctional alkoxy silane [24]. The reaction is usually conducted in aqueous or hydro-alcoholic media. The important steps in silanization are [25]: (i) silane hydrolysis which leads to  $\text{R-Si(OH)}_3$ , (ii) hydrogen bonding between the hydrolysed silane and the surface, (iii) condensation with the surface resulting in surface-O-Si linkage, (iv) possible polymerization of the silane in solution, and (v) reaction with pending R group with other species as will be briefly discussed below.

In the case of biochar, the abundance of -OH functional groups is crucial for its functionalization with silane coupling agents. Such a modification permits to fabricate high performance biochar-filled polymer composites, immobilized catalysts and metal complexes, materials for electromagnetic shielding and road engineering among numerous applications. We will select a few case studies of distinct types of applications in order to show the possibilities offered by silanes to impart new functionalities and performances to biochar.

Figure 2a depicts a general pathway of functionalization of biochar bearing surface hydroxyl groups. The group R borne by the silane is chosen in a way it imparts a specific functionality to biochar: post-functionalization, hydrophilic/hydrophobic interactions, metal complexation/chelation, in situ polymerization, dispersion in polymer matrix. Indeed, modified biochar can be used to make composite membrane for pervaporation, a process that uses a poly(dimethyl siloxane) (PDMS) for separation ethanol/water mixture [26]. Figure 2b shows the steps involved in biochar silanization. Firstly, silanes go through hydrolysis, followed by condensation to produce oligomers. Finally, oligomers react with -OH groups on biochar surface, thus leading to biochar-O-Si covalent bonds [27]. Pending methoxy groups react with PDMS which results in

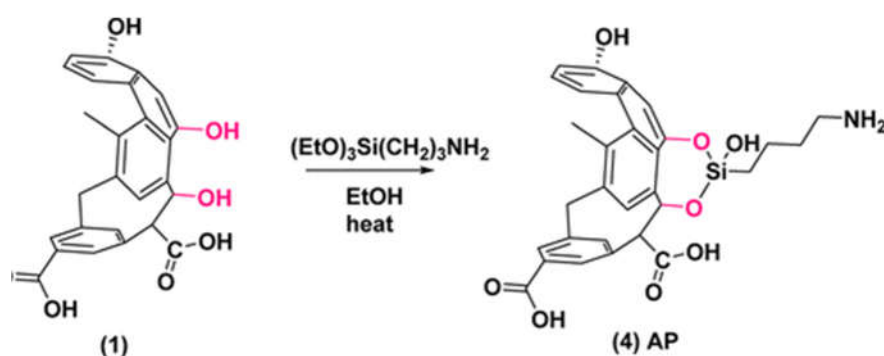


biochar/PDMS composite membrane. Vinyl-silanized biochar imparts superior hydrophobic properties to the PDMA membrane compared to aminosilane, as the latter interacts favourably with water due to its free amine group [26].



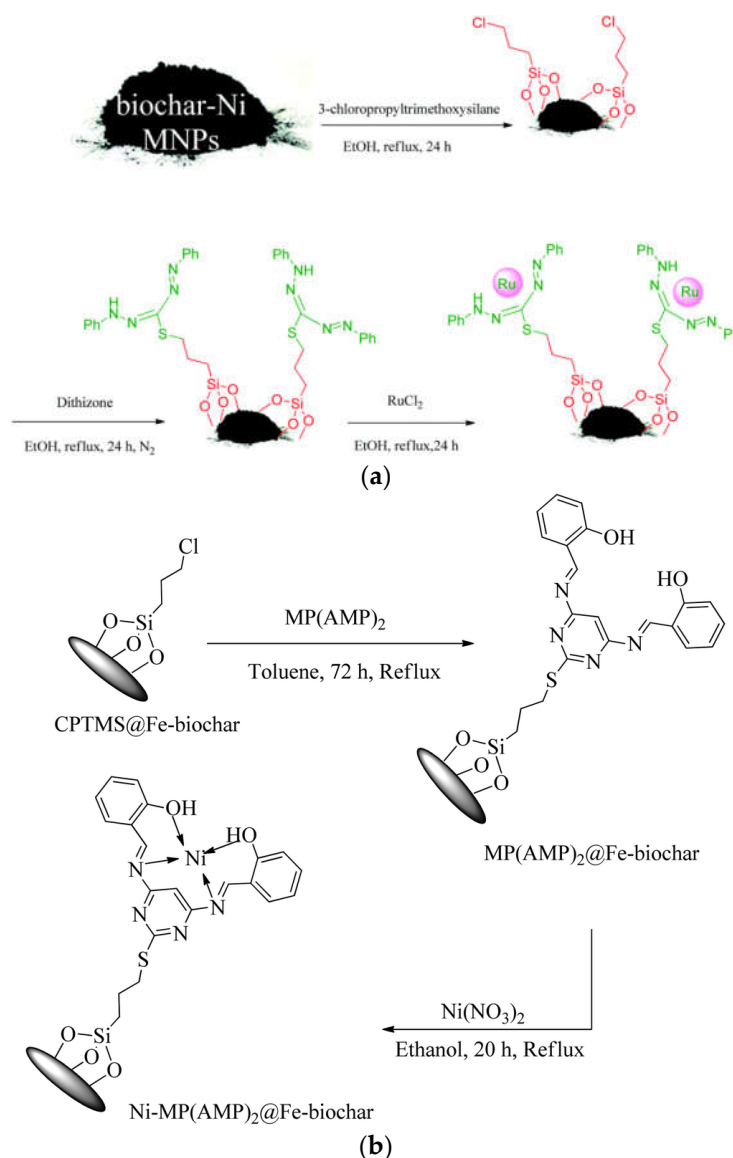
**Figure 2.** (a). General pathway for the silanization of biochar. R=  $-(\text{CH}_2)_3\text{NH}_2$ ,  $-(\text{CH}_2)_3\text{Cl}$ ,  $-(\text{CH}_2)_3\text{SH}$ ,  $-(\text{CH}_2)_3\text{O}-(\text{C}=\text{O})-(\text{C}=\text{CH}_2)\text{CH}_3$ ,  $-\text{CH}=\text{CH}_2$ . (b) Silanization of wood biochar with vinylsilane, followed by reaction with PDMS. Reproduced from [26] with permission of John Wiley & Sons.

Silanization of the surface with aminosilane (Figure 3), followed by condensation, led to a removal capacity of  $\text{CO}_2$  3.7 mmol/g (specific surface area  $\text{SSA}=394\text{ m}^2/\text{g}$ ), higher than 3.4 mmol/g, obtained with Norit, a commercial product of which  $\text{SSA}=3.4\text{ mmol/g}$  [28].



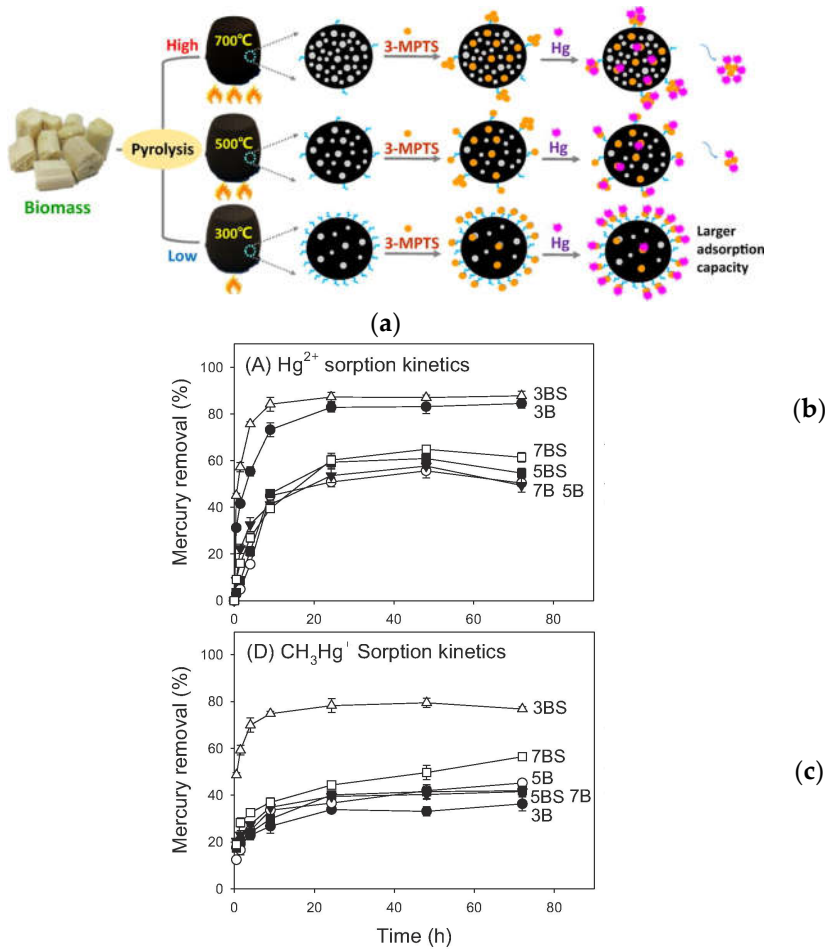
**Figure 3.** Modification of biochar surface with aminosilane coupling agent. Reproduced from [28] with permission of ACS.

Silanization could be an important step to enable post-functionalization of biochar, with complex structure such as metal chelators. Figure 4 depicts a strategy for anchoring ruthenium (Figure 4a), iron and nickel containing moieties (Figure 4b). They have exhibited enhanced catalytic activity with high turnover frequency for organic reactions.



**Figure 4.** Strategies to design silanized biochar for the immobilization of heterogeneous catalysts of organic chemical reactions: Biochar@Ni modified with silane for covalent coupling of ruthenium ligand (a), and chloro-silanized biochar, post-modified with mercaptan derivative for chelating nickel catalyst (b). (a) Reproduced with permission of RSC, from [29] (a), and from [30] (b).

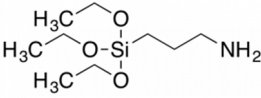
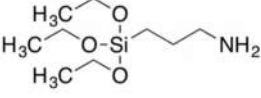
If silanization permits to impart new functionality to biochar, spatial distribution of the surface bound reactive groups is an issue. For example, Huang *et al.* [31] have brought strong supporting evidence for the effect of pyrolysis temperature on the silanization extent of pine sawdust biochar; they have shown that mercapto-silanization was more efficient with the decreasing order of temperature  $300 > 500 > 700$  °C. Indeed, biochar has much more OH, C=O and COOH groups at low pyrolysis temperature, therefore enabling even distribution of SH groups at the surface, resulting in larger removal of  $Hg(II)$  and  $\alpha HCHg^+$  ions (Figure 5). Interestingly, the high resolution S2p region from 3BS biochar (prepared at 300 °C and silanized) exhibited peak broadening due to the formation of mercury sulphide. Although 3B and 3BS samples exhibited lowest specific surface area (1.7 and 4.2  $m^2/g$ , respectively), substantial mercury compounds could be removed (see Figure 5b,c). This is clear indication that even and densely packed distribution of mercapto groups overcame the textural properties imparted by high pyrolysis temperature (335 and 235  $m^2/g$  for 7B and 7BS, respectively).

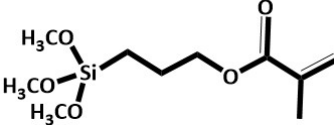
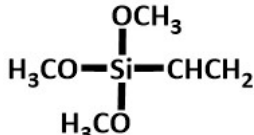
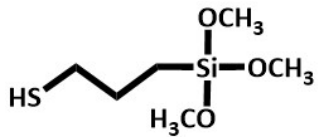
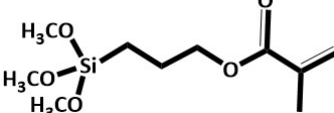
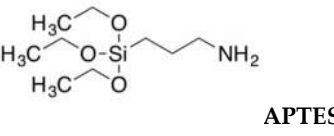
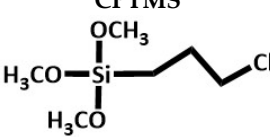
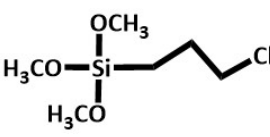


**Figure 5.** Fabrication of mercapto-silanized biochar for the removal of Hg compounds. Schematic illustration of the pyrolysis temperature effect on silanization extent, textural and adsorption capacity of biochar (a); effect of pyrolysis temperature and silanization on the removal of Hg<sup>2+</sup> (b), and <sup>3</sup>HCHg<sup>+</sup> (c). Reproduced from [31] with permission of Elsevier.

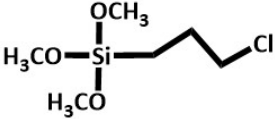
Table 2 reports different silane coupling agents employed to modify biochar surface and their potential applications. It shows that either as such silane modified biochar or their further modification have been used for different purposes including water treatment, nanoparticles capture, polymer reinforcement, membranes, road engineering, land fill cover, etc.

**Table 2.** Surface treatment of biochar with silanes coupling agents.

Coupling agent	Biomass	Surface treatment conditions	Properties of engineered biochar	Potential application	References
	Sawmill residues	Char/water=10/1; 2 wt.% APTES; condensation at pH 3-4 for 1h followed by reaction at 70 °C for 6h. Post-activation in air at 560 °C.	SSA=394 m <sup>2</sup> /g; 0.24 wt.% N;	CO <sub>2</sub> adsorption capacity of 3.7 mmol/g	[28]
 KH-550	Oil sludge	C <sub>2</sub> H <sub>5</sub> OH: H <sub>2</sub> O: KH-550 ratio of 70: 25: 5, left for 60 min. Then, oil sludge pyrolysis residue added and stirred for 1 h, followed by drying at 60 °C.	Rheological properties (rutting resistance factor, creep stiffness, and high temperature performance) improvement of the asphalt mortar	Road engineering	[32]

<p>KH-570</p> 	Rice straw	Mixture of pre-treated biochar + 20% (v/v) KH-570, 72% (v/v) absolute C <sub>2</sub> H <sub>5</sub> OH + 8% (v/v) H <sub>2</sub> O, magnetically stirred at 30°C, mixed with modifier for 12h, washed with ethanol, filtered and dried at 50°C.	Enhanced CH <sub>4</sub> oxidation	Soil cover for landfill gas control.	[33]
<p>YDH-171</p> 	lodgepole pine bark	Synthesized biochar at 600°C and modified by YDH-171. Further, 3 wt.% modified were taken for further experiment	PV performance: separation factor (11.3) and flux (227.25 g m <sup>-2</sup> h <sup>-1</sup> ).	PV membranes (Separating C <sub>2</sub> H <sub>5</sub> OH from H <sub>2</sub> O.	[26]
<p>A-189</p> 	Bamboo	Pre-treated ultrafine bamboo char was mixed with A-189 (16 w/w%). Following silane treatment, oven-dried for 24 at 105 °C.	Tensile strength (18.87 MPa) and tensile modulus (272 MPa) increased by 99.3 % and 104.9%).	Polymer reinforcement	[34]
<p>KH-570</p> 	Rice straw	-	H <sub>2</sub> O absorption = 1.27 g (g biochar) <sup>-1</sup> Water proofing, MOB growth promotion, ventilation and efficient CH <sub>4</sub> reduction.	Land fill cover soil	[35]
<p>APTES</p> 	Onion peels	Silane (3 wt.%) was mixed with C <sub>2</sub> H <sub>5</sub> OH- H <sub>2</sub> O solution (95 wt % C <sub>2</sub> H <sub>5</sub> OH + water + acid 5%), stirred for 10 at room temp. Then, ball milled Co-biochar was incorporated, rinsed for 10 min and filtered, and finally dried at 110°C.	High tensile strength and EMI: -44.37 dB and - 49.62 dB for X and Ku band	PVA composite For EMI application	[36]
<p>CPTMS</p> 	Chicken manure	Pyrolyzed biomass (400-800 °C, 1 to 2h) was treated with CPTMS followed by dispersion in 1.5 mmol TBA and toluene and stirred for 48 h at 90°C. Residue was isolated, washed with C <sub>2</sub> H <sub>5</sub> OH and dried (50°C). Then, Pd (OAc) and NaBH <sub>4</sub> treatment at optimum condition.	In the synthesis of biphenyl derivatives (yield = 97%, TON = 135, and TOF = 405)	C-C coupling reaction (Suzuki-Miyaura and Heck-Mizoroki cross-coupling reactions.)	[37]
	Chicken manure	Biochar-Ni magnetic composite were refluxed with 1.5 silane in the presence of ETOH for 24 h. Several other steps followed by treatment with dithizone and RuCl <sub>2</sub> leads to formation of Ru-dithizone@biochar-Ni MNPs	High catalytic activity for C-C coupling reaction of iodobenzene or chlorobenzene with 96 % yield.	Suzuki C-C coupling reaction	[29]



	Chicken manure	CPTMS@Fe-biochar treated with MP(AMP)2 and refluxed for 72 h in the presence of toluene and then the product is refluxed with ethanol and nickel nitrate for 20h.	Enhanced catalytic efficiency. Catalyst recovery through magnet. Homoselectivity was observed. %yield = 98%. Recyclable upto 9 times.	Catalysis ( synthesis of tetrazole derivatives)	[30]
---	----------------	---	---	---	------

APTES: aminopropyl triethoxysilane; EMI: electromagnetic interference shielding; PV: Pervaporation ; PVA: Poly vinyl alcohol; SSA: specific surface area; TOF: turnover frequency.

### 2.3. Titanate Surface Modifiers

Titanates are well known coupling agents in composite science and technology [38,39]. generally speaking, and more specifically in the domain of dental materials [40,41]. They are proposed for the fabrication of robust dental composite materials.

They have been explored in surface modification of rice bran biochar, but without mention of potentially occurring surface reaction [22]. For this purpose, magnetic biochar was prepared by post-modification with Fe(II) and Fe(III) iron chlorides via pyrolysis, followed by sol-gel process synthesis of TiO<sub>2</sub> from titanate, in the presence of the magnetic biochar@Fe. The final material was applied for the photocatalyzed removal of tetracycline antibiotic, and for antibacterial application. Of particular interest to surface and interface phenomena, Ti-O-C interfacial functional group was probed by FTIR, which accounts for covalent attachment of TiO<sub>2</sub> to the underlying biochar.

In another study, titanate were used in order to modify preformed biochar in a sol-gel process. The titanate-modified biochar was pyrolyzed in order to obtain biochar@TiO<sub>2</sub>. Further wetting impregnation with silver nitrate followed by pyrolysis resulted in biochar@TiO<sub>2</sub>-Ag with antibacterial activity against *E. coli* (99% of sterilization ratio in 5 min, under daylight) [42].

XPS analysis was used to probe titanate interaction with carbon allotropes, but only rare examples have been found. For example, activated carbon was treated with titanate in order to design supercapacitors (specific capacitance: 376.2 F.g<sup>-1</sup>, internal resistance: 0.91 Ω) [43].

Although, not strictly on biochar, but of relevance to this review and the scope of the journal Surfaces, recently titanates were proposed for the covalent attachment of graphene oxide (Figure 6) in order to provide surface-bound alkyl groups that ensure dispersion of GO in hydraulic oils [44]. Interestingly, C1s spectra show drastic decrease of C-O component due to the covalent attachment of the long alkyl chains to the GO via titanium. Such surface-bound groups permitted excellent dispersion of titanate-modified GO in hydraulic oil with remarkably improved tribological properties.

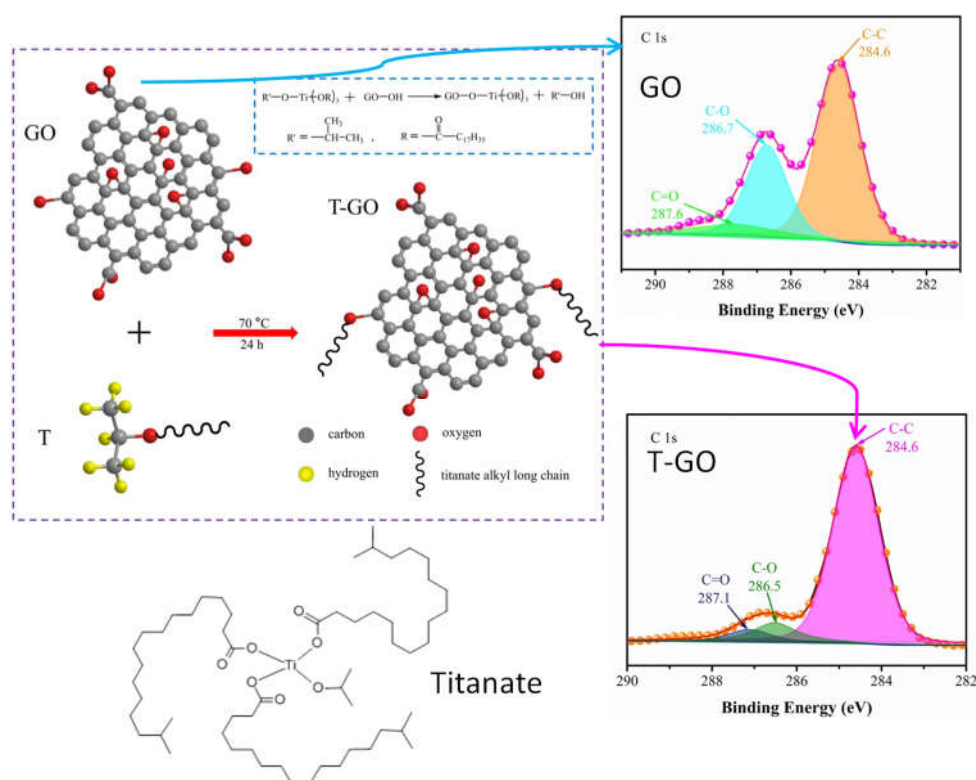


**Figure 6.** Covalent modification of graphene oxide with isopropyl triisostearyl titanate. Reproduced from [44] with permission of Elsevier.

#### 2.4. Modification of Biochar by Ionic and Nonionic Surfactants

Biochar surface properties could be changed through modification with the surfactant layers. The ionic and non-ionic surfactant adsorbed on the solid surface influence the specific surface area, content of acidic-basic functional groups and hydrophobic properties of these materials. Various mechanisms of surfactant molecules binding can be involved in such kinds of systems. The electrostatic interactions, hydrogen bonds, interactions between the  $\pi$ - $\pi$  electrons, bilayer formation and hydrophobic interactions are associated with the surfactants adsorption which is schematically presented in Figure 7.

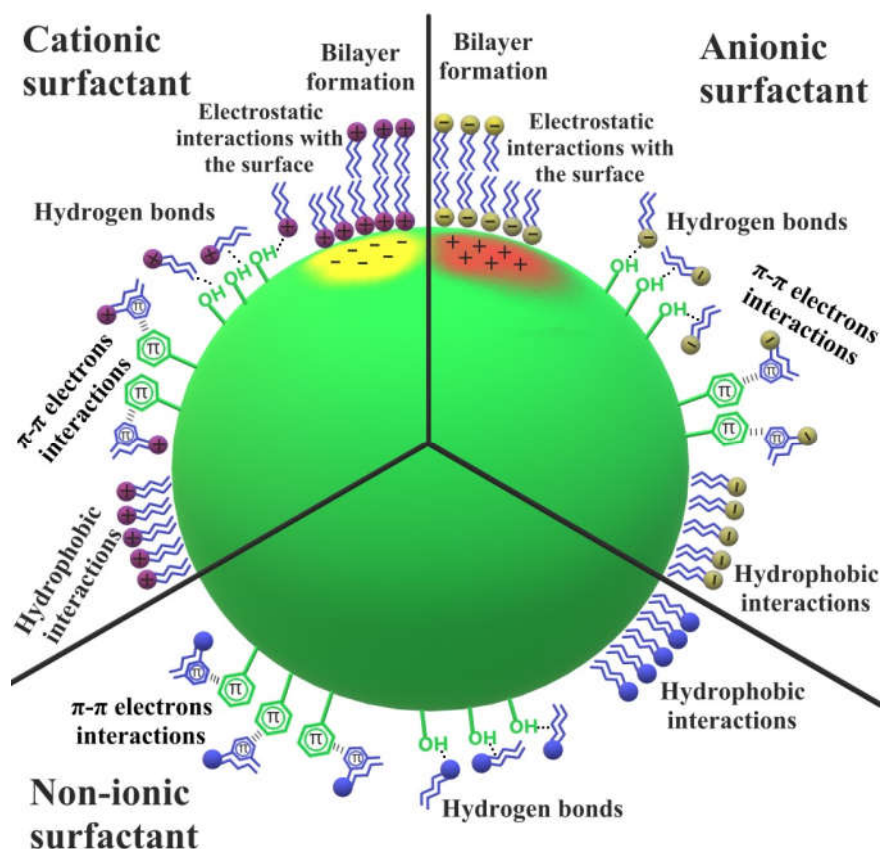


**Figure 7.** Possible adsorption mechanisms of surfactants with various ionic character on biochar surface.

These modifications with the surface active agents can both increase and decrease the biochar adsorption capacity, depending on the adsorbate and surfactant chemical character. The adsorption phenomenon could take place due to the all above mentioned mechanisms. Moreover, the surfactant-adsorbate multilayers creation and the micelles formation have a positive effect on the adsorbed amounts of inorganic and organic substances (Figure 8).

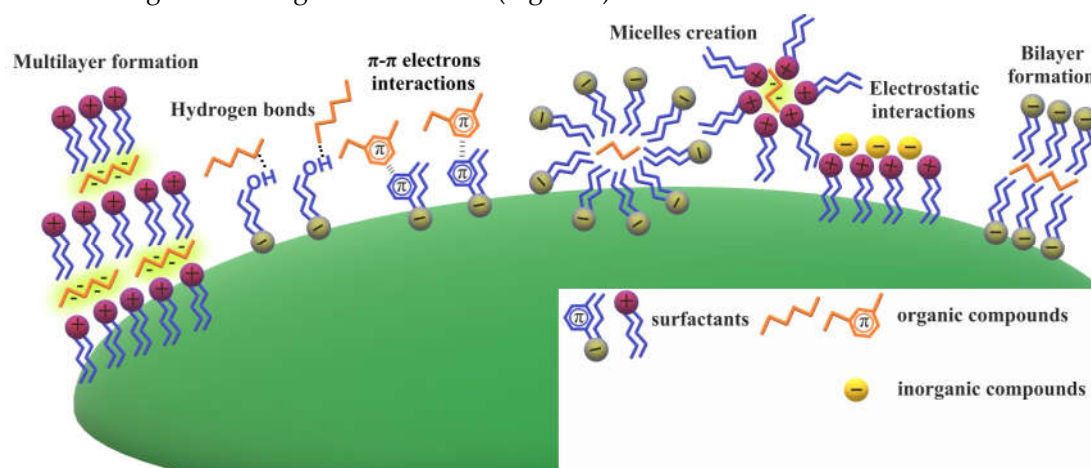


**Figure 8.** Possible mechanisms of organic and inorganic compounds adsorption on surfactant-modified biochar surface.

Biochar obtained from the *Populus alba* tree was modified with the cationic surfactant, cetyltrimethyl ammonium bromide (CTAB) and used for Cr(VI) adsorption. The obtained results proved that the surfactant modification affects the Cr(VI) adsorption favourably. The adsorbed

amount increases on the of modified biochar surface in comparison with the non-modified one independently of the adsorbent dose [45]. CTAB was also used for the biochar derived from the rice husk. The obtained results showed that due to the modification of adsorbent, its surface charge change to be positive. The modified biochar was used for inorganic nitrogen fertilizers removal from the aqueous solution. The removal percentage increased by 13 % in the case of the modified adsorbent application in comparison to the non-modified material [46].

The cationic CTAB modification was also performed in the case of the activated biochars obtained from the peanut shells and corncobs used for the anionic polymer - poly(acrylic acid) (PAA) adsorption. The surfactant modification favoured the increase of the polymer adsorption amount on both examined adsorbents. The poly(acrylic acid) removal from the aqueous solution is strongly related to its pH value, however, at all examined pH values (3, 6, 9), the anionic polymer is better adsorbed on the surface of the CTAB-modified activated biochar. In such a case the maximum PAA adsorbed amount was 68 mg/g [47].

The CTAB-modified biochar obtained from the peanut shells and corncobs were likewise used for the Bisphenol A adsorption. The pyrolysis was performed at 300, 500 and 700 °C. It was found that the CTAB modification inhibits the Bisphenol A adsorption and this effect becomes stronger with the increasing pyrolysis temperature. It was also proved that the higher the surfactant concentration was applied, the smaller adsorbed amount of Bisphenol was found [48].

The CTAB-modified coffee husk activated biochar was used for the reactive dyes removal from the aqueous solution. The reactive yellow 145 (RDY145) dye adsorbed amount was the largest on the surface of the CTAB-modified activated biochar in comparison to two commercially available different non-modified activated carbons. The pH value has no significant effect on the RDY145 adsorbed amount. The Reactive Red 195 and Reactive Blue 222 dyes were also effectively separated from the aqueous system [49]. The other studies deal with the adsorption of Orange II (OII) and Methylene Blue (MB) dyes on the CTAB-modified biochar obtained from the cornstalk. Due to the adsorbent charge changes to positive (the non-modified biochar has a negative surface charge), the adsorbed amount of positively charged methylene blue decreases. In turn, the adsorbed amount of negatively charged OII increases compared to that observed for non-modified biochar. These effects are related to the electrostatic adsorption mechanism. The obtained maximum removal using the modified biochar was 40 % for methylene blue and 100 % for OII.[50]

The anionic surfactant, sodium dodecyl benzene sulfonate (SDBS) was used for the surface modification of the biochar obtained from the rice husk. The modified adsorbent was used for the inorganic nitrogen fertilizers removal from the aqueous solution. It was proved that the surfactant modification increases the removal efficiency by 2 % compared to the non-modified biochar [46].

Sodium dodecyl sulfate (SDS) is an anionic surfactant which was used for modification of activated biochars obtained from the peanut shells, corncobs and peat. All above-mentioned adsorbents were used for the poly(acrylic acid) adsorption. The experiments indicated that the SDS modification effect on the PAA adsorbed amount depends largely on the adsorbent type and the solution pH value. On the surface of the activated biochars obtained from the peanut shells and corncobs, poly(acrylic acid) adsorption was inhibited at pH 9, however at pH 3 and 6 the surfactant modification affect the polymer adsorbed amount favourably. This is probably related to the PAA conformation change at different pH values. The maximum removal was 60 % [47]. Moreover the SDS modification reduced largely the PAA adsorbed amount at pH 4.5, 6 and 9 on the surface of activated biochar derived from the peat compared to the non-modified one. However at pH 3 the modification did not affect significantly the polymer removal, which remained in the amount over 90 % [51].

The anionic SDBS surfactant was used for modification of the biochar derived from the peanut shells. The obtained biochar was used for the Bisphenol A adsorption. It was proved that the SDBS modification affects the Bisphenol A adsorbed amount negatively. The inhibition became stronger and stronger with the increasing surfactant concentration. The Bisphenol A adsorbed amount on the surface of the non-modified biochar was 100 mg/g and on the surface of SDBD-modified biochar 10 mg/g [48].

The biochar obtained from the cassava peels was modified with the SDBS and SDS surfactants and used for the methylene blue adsorption. It was proved that the SDBS modified sample resulted in a larger number of the surface active sites and increased the dye adsorbed amount. In the case of SDS, due to the changes of the adsorbent surface charge to negative, it had the favourable impact on the dye adsorbed amount increase [52,53]. MB was also adsorbed on the surface of the SDS-modified biochar obtained from the peanut shells. The adsorbent was modified with SDS of different concentrations. The obtained results showed that with the increasing surfactant concentration, the surface area accessible to adsorption increases. As a result the methylene blue adsorbed amounts were considerably larger. The maximum adsorption capacity of the SDS-modified biochar as regards MB was 503 mg/g [54].

The SDBS and SDS anionic surfactants were applied for the magnetic biochars derived from the corncobs and furfural residue modification. The obtained adsorbents were used for the norfloxacin (an antibiotic with the bactericidal action) adsorption. It was proved that the surfactant modification increased the norfloxacin adsorbed amount. The SDBS with a small concentration showed a larger impact on the antibiotic adsorption whereas SDS with higher concentrations was more effective [21].

Magnetic biochars modified with the amphoteric surfactant - dodecyl dimethyl betaine (BS-12) were used for the phenanthrene adsorption. The adsorbed amount of phenanthrene BS-MC (substance from the group of polycyclic aromatic hydrocarbons) decreased with the increasing BS-12 surface coating ratio. The change in the solution pH values caused no significant effects on the phenanthrene adsorption [55].

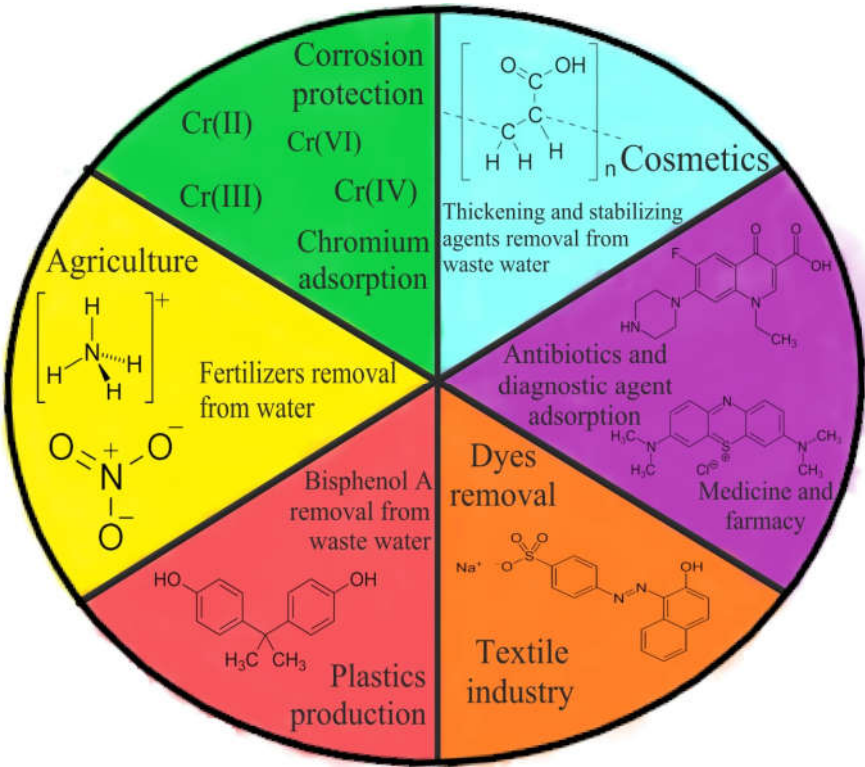
Triton X-100 (2-[4-(2,4,4-trimethylpentan-2-yl)phenoxy]ethanol) belongs to the group of non-ionic surfactants. It was used for the activated biochar derived from the horsetail herb modification. The obtained adsorbent was successfully applied for the poly(acrylic acid) polymer and toxic Pb(II) heavy metal adsorption from the aqueous solutions. It was shown that the PAA adsorbed amounts decrease on the surface of the modified biochar compared to the non-modified one whereas the Pb(II) adsorption is more effective on the surface of the Triton X-100-modified adsorbent.[56] Poly(acrylic acid) was also adsorbed on the surface of the activated biochars obtained from the peanut shells and corncobs, modified with Triton X-100. The surfactant modification had a small impact on the PAA adsorbed amount. Moreover, the changes in the solution pH values (3, 6, 9) influenced the poly(acrylic acid) adsorbed amount more significantly compared with any adsorbents modifications with the surface active agent. The obtained maximum adsorbed amount of PAA on the Triton X-100-modified activated biochar was 55 mg/g [47].

The biochars obtained from the peanut shells used for the Bisphenol A removal, were modified with the non-ionic surfactant Tween 20 (polyoxyethylene (20) sorbitan monolaurate). Its effect on Bisphenol A adsorbed amount was similar to that caused by the ionic surfactants (CTAB, SDBS). The adsorbed amount decreased 10 times on the surface of the Tween 20-modified biochar in comparison to the non-modified one. The adsorption efficiency decreased with the increasing concentration of Tween 20 [48].

After the chemical activation the biochars obtained from the eucalyptus sawdust were modified with the three different non-ionic surfactants: PEG 2000 (polyethylene glycol), Pluronic P-123 (poly(ethylene glycol)-*block*-poly(propylene glycol)-*block*-poly(ethylene glycol)) and Pluronic F-127 (2-[2-(2-hydroxyethoxy)propoxy]ethanol)) and used for the adsorption of metronidazole (an antibiotic used to treat infections with anaerobic microorganisms and mixed flora with anaerobes). All of the examined surfactants (dissolved in ethanol) affected the solid porous structure. PEG 2000 and Pluronic P-123 increased the pore volume and its mean diameter whereas Pluronic F-127 enhanced only the pore size. All the above surfactants had the impact on the metronidazole adsorption. The antibiotic exhibited the greatest affinity for the surface of the adsorbent modified with PEG 2000 (removal 100 %) whereas its adsorbed amount was the smallest on the surface of the Pluronic F-127-modified biochar (removal 80 %) [57].

Table 3 summarizes the experimental conditions for the design and salient features of surfactant-modified biochar specimens, whereas Figure 9 presents the possible applications of surfactant-modified biochars.

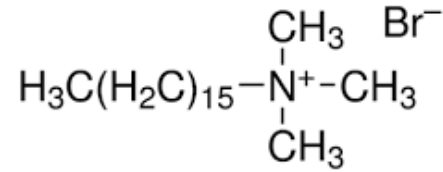


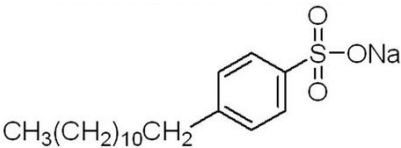
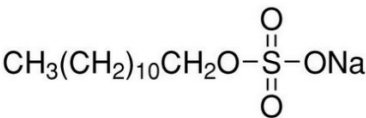
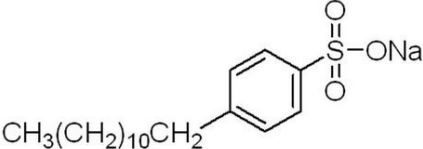
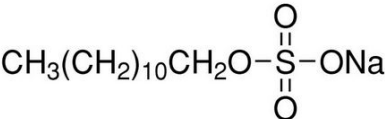
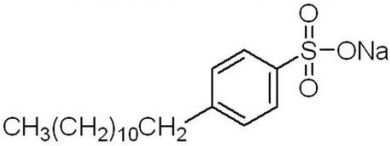
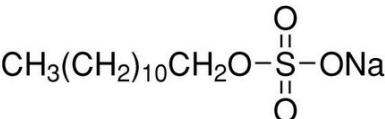
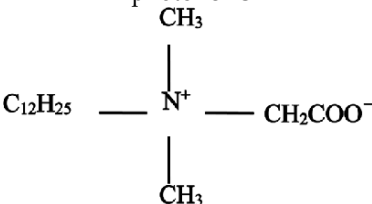


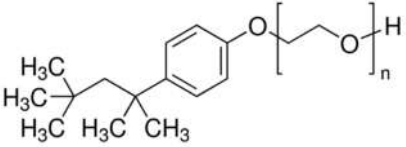
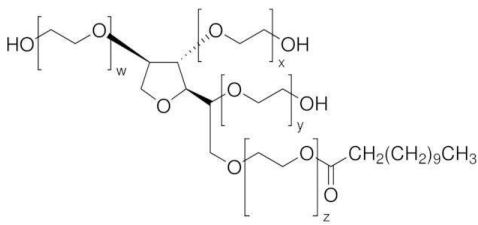
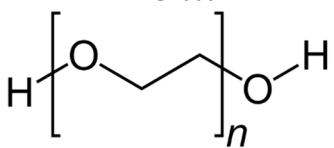
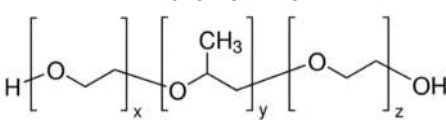
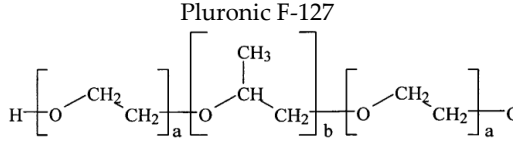
**Figure 9.** Applications of biochars modified by surfactants in various fields of human activity.

**Table 3.** Summary of inorganic and organic compounds adsorption on the surfactant-modified biochar surface.

Surfactant	Biomass used for biochar preparation	Surfactant immobilization conditions	Properties of modified biochar	Application	Reference
Cationic CTAB	<i>Populus alba</i>	Co: 22 mg/L Dried at 105 °C	-	Cr(VI)	[45]
	Rice husk	Co:1457 mg/L Dried at 60 °C	Surface charge change to positive	Inorganic nitrogen fertilizers removal	[46]
	Peanut shells Corncobs	Co: 100 mg/L pH=3, 6, 9	-	Poly(acrylic acid) adsorption	[47]
	Peanut shells	Co: 17-272 mg/L T: 25 °C pH: 6	-	Bisphenol A adsorption	[48]
	Coffee husk	Co: 2550 mg/L T: 30 °C Dried at 60 °C	Specific surface area decrease (from 750.1 to 557.4 m²/g) Pore volume decrease (from 0.3541 to 0.3192 cm³/g) Pore mean diameter increase (from 18.9 to 22.9 Å)	Reactive dyes removal	[49]



	Cornstalks	C <sub>0</sub> : 10 mg/L Dried at 60 °C Neutral pH	Surface charge change to positive	Orange II and methylene blue adsorption	[50]
Anionic SDBS 	Rice husk	C <sub>0</sub> : 437.5 mg/L Dried at 60 °C	Surface charge change to negative	Inorganic nitrogen fertilizers removal	[46]
Anionic SDS 	Peanut shells Corncobs	C <sub>0</sub> : 100 mg/L pH: 3, 6, 9	-	Poly(acrylic acid) adsorption	[47]
	Peat	C <sub>0</sub> : 100 mg/L pH: 3, 4.5, 6, 9	-	Poly(acrylic acid) adsorption	[51]
Anionic SDBS 	Peanut shells	C <sub>0</sub> : 24.5-392 mg/L T: 25 °C pH: 6	-	Bisphenol A adsorption	[48]
	Cassava peels	C <sub>0</sub> : 30-150 mg Dried at 110 °C	More numerous surface active sites availability	Methylene blue adsorption	[52]
	Cassava peels	C <sub>0</sub> : 30-150 mg/L Dried at 110 °C	-	Methylene blue adsorption	[53]
Anionic SDS 	Peanut shells	C <sub>0</sub> : 6-30 mg/L Dried at 65 °C	Specific surface area increase (from 51.37 to 85.62 m <sup>2</sup> /g) Pore volume increase (from 0.232 to 0.283 cm <sup>3</sup> /g) Pore mean diameter decrease (from 3.794 to 1.543 nm)	Methylene blue adsorption	[54]
Anionic SDBS 	Corncob Furfural residue	C <sub>0</sub> : 61.25-3062.5 mg/L pH: 2-10		Norfloxacin adsorption	[21]
Anionic SDS 	Corncob Furfural residue	C <sub>0</sub> : 61.25-3062.5 mg/L pH: 2-10		Norfloxacin adsorption	[21]
Amphoteric BS-12 	-	Modification 25-200 %	-	Phenanthrene adsorption	[55]

 <p>Non-ionic Triton X-100</p>	Horsetail herb	C <sub>0</sub> : 100 mg/L pH: 3	-	Poly(acrylic acid) and Pb(II) adsorption	[56]
	Peanut shells Corncobs	C <sub>0</sub> : 100 mg/L pH: 3, 6, 9	-	Poly(acrylic acid) adsorption	[47]
 <p>Non-ionic Tween 20</p>	Peanut shells	C <sub>0</sub> : 3.5-56 mg/L T: 25 °C pH: 6	-	Bisphenol A adsorption	[48]
 <p>PEG2000</p>	Eucalyptus sawdust	Surfactant dissolved in ethanol T: 60 °C Neutral pH	Specific surface area decrease (from 462 to 448 m <sup>2</sup> /g) Pore volume increase (from 0.309 to 0.392 cm <sup>3</sup> /g) Pore mean diameter increase (from 2.679 to 3.497 nm)	Metronidazole adsorption	[57]
 <p>Pluronic P-123</p>	Eucalyptus sawdust	Surfactant dissolved in ethanol T: 60 °C Neutral pH	Specific surface area decrease (from 462 to 436 m <sup>2</sup> /g) Pore volume increase (from 0.309 to 0.3586 cm <sup>3</sup> /g) Pore mean diameter increase (from 2.679 to 3.289 nm)	Metronidazole adsorption	[57]
 <p>Pluronic F-127</p>	Eucalyptus sawdust	Surfactant dissolved in ethanol T: 60 °C Neutral pH	Specific surface area decrease (from 462 to 221 m <sup>2</sup> /g) Pore volume decrease (from 0.309 to 0.2465 cm <sup>3</sup> /g) Pore mean diameter increase (from 2.679 to 4.466 nm)	Metronidazole adsorption	[57]

### 2.5. Surface Arylation with Diazonium Salts

The chemistry of aryl diazonium salts dates back to the mid-1800s [58] and was at the origin of the industrial production of azo dyes [59]. It is also explored in numerous organic synthesis reactions [60]. Only since 1992 it became world-wide applied to modify materials surfaces, particularly carbon

allotropes [20,61]. This approach is alluring because of its commercially abundant comprising aromatic amines with various functional groups, as diazonium precursors.

A general pathway for the modification of carbon materials is depicted in Figure 10. Mostly, the *ex-situ* or *in-situ* generated diazonium salt reacts in aqueous or organic solvents in order to provide radicals that attack the surface, or the diazonium forms diazoether interfacial bond, followed by release of dinitrogen and formation of C-O-C interface. Example is given for carbon surface bearing surface functional groups.

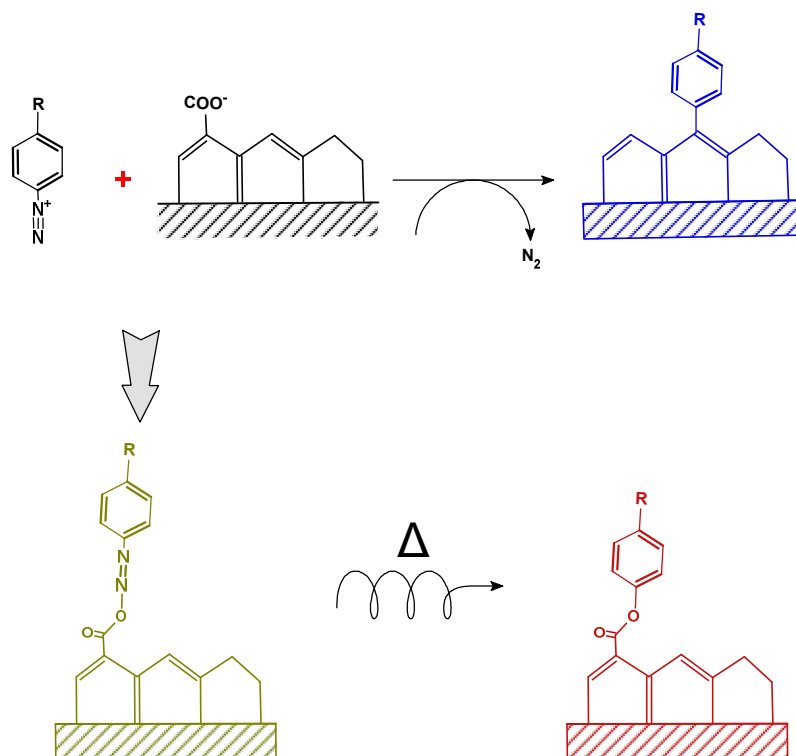


**Figure 10.** Schematic illustration of the modification of a graphitic surface with aryl diazonium salts.

Biochar is among these functionalized carbons and is thus prone to arylation with diazonium salts. The grafted aryl groups display scaffolds to link moieties through specific reactions as they possess suitable functional groups. They comprise amide coupling, coordination bonding and click chemistry [55]. The surface-aryl bond is usually strong owing to its covalent nature, therefore ensuring remarkable mechanical properties of polymers reinforced with arylated fillers, or strong adhesive bonding of polymers to arylated surfaces. One can also take advantage of the strong arylation of carbonaceous supports to anchor bimetallic nanocatalysts, with excellent dispersion and narrow size distribution for nitrate electroreduction application [62].

The arylation of carbon allotropes including fullerene, graphene and carbon nanotubes with diazonium salts showed enhanced properties and performances in several domains such as electrocatalysis, sensing, and optics [55]. However, these precursors are expensive with limited large scale applications. Alternatively, the obtained biochar from agrowastes pyrolysis can provide a highly porous matrix compared to the initial lignocellulosic materials [63]. Biochar can be treated with acids or alkalis to provide higher surface area with enhanced porous structure. Apple leave-derived char was activated through various processes. This work study was concerned with investigating the impact of acid and thermal treatments on the physico-chemical properties of the resulting biochar. The latter was capable of abstracting the organic pollutants from water [64]. Several Raman spectra for carbonaceous matters seem to be complex. It may be referred to the complicated structure they possess. The simplest spectrum is for graphite because of the uniformity of its formation showing planar and stratified laminates. Relative deformations may arise in this structure expressing a weak D band with a directly proportional intensity to the extent of disorders in this

structure. Khalil et al.[65] investigated fundamental variations in the D/G peak intensity ratio on going from the pristine biochar derived from pomegranate peels when compared to different arylated biochar samples; namely Biochar-COOH, biochar-SO<sub>3</sub>H and biochar-Azure A. The results expressed that D/G peak ratio grows with arylation without depending on the kind of the diazonium compound. The intensity of Raman D/G peaks was correlated to the elementary concentration of the employed diazonium salts. Figure 11a depicts the general route for arylation of pomegranate biochar with in situ generated three diazonium salts. Figure 11b compares the Raman bands of pristine and arylated biochar; the D/G intensity ratio increases upon treatment of diazonium salts, which a sign for true covalent modification resulting from arylation. Figure 11c plots D/G ratio as a function of the grafting extent determined by TGA. Interestingly, for similar high initial concentration, Azure A induces marginal change in D/G intensity ratio due to steric hindrance. Figure 11d schematically illustrates the gradual change in the grafting density of aryl groups at the surface. High initial concentration is likely to result in oligomerization of the aryl groups, [56,66] hence the tendency of the D/G intensity ratio to reach a plateau value. Indeed, chemical grafting reactions no longer affect the carbon allotrope support, but the organic layer, previously attached [67].

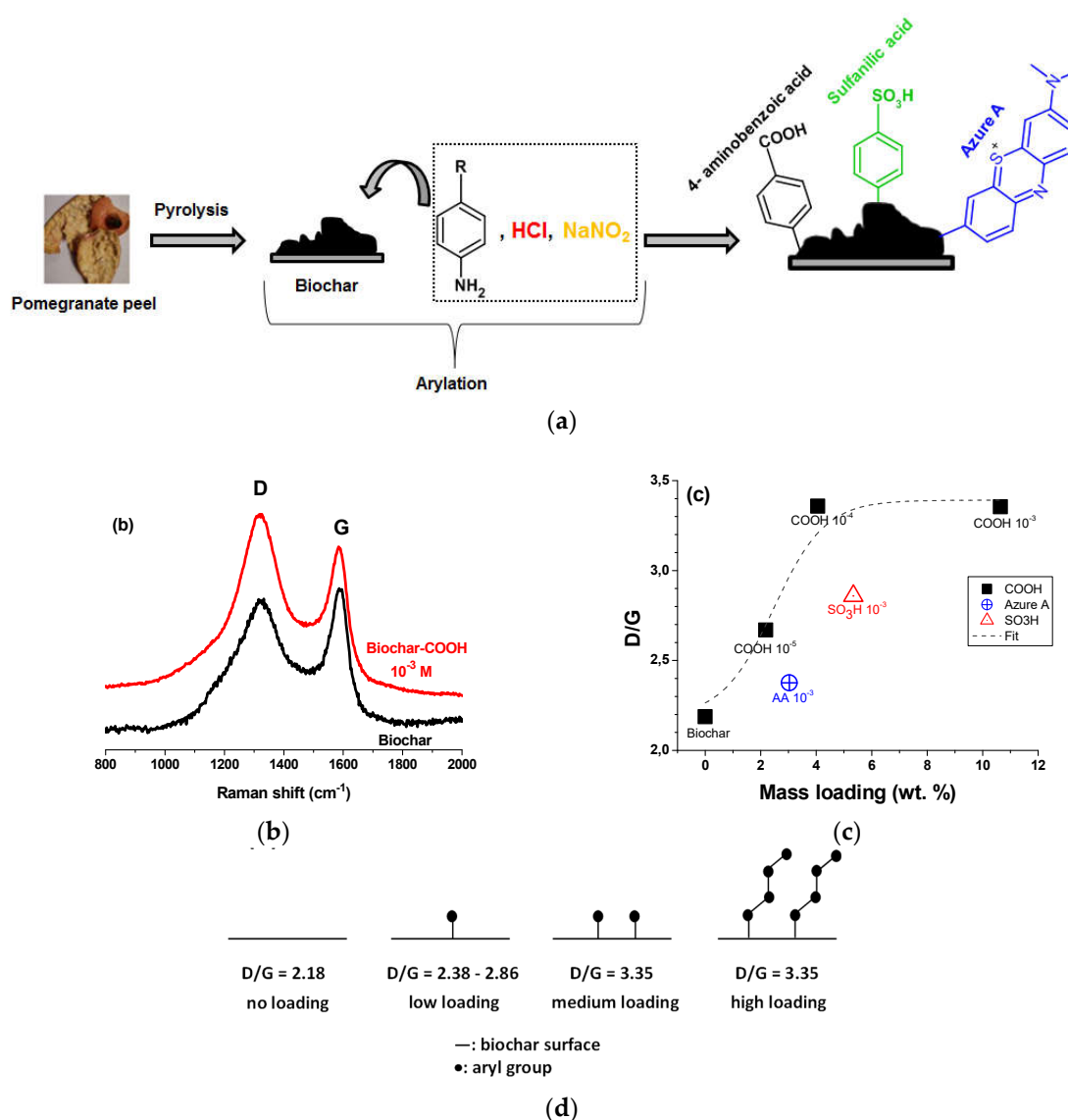
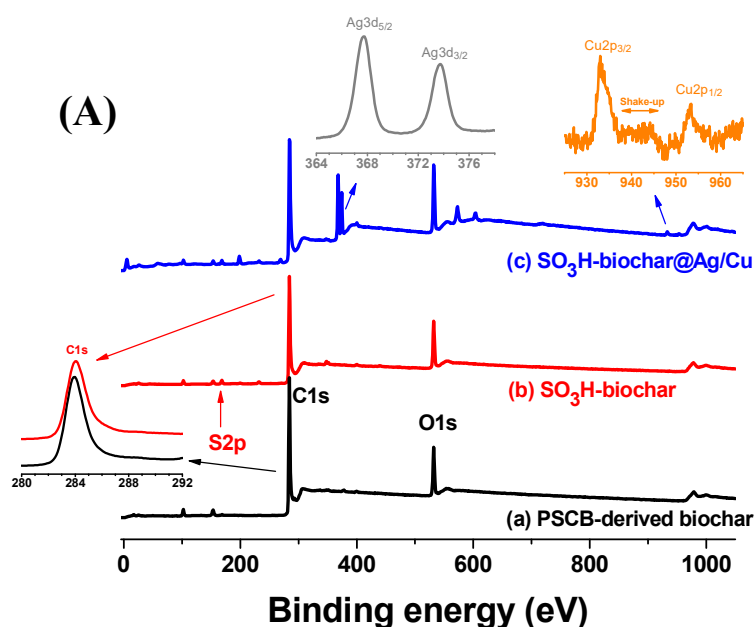


**Figure 11.** Arylation of pomegranate biochar: (a) modification with in situ generated diazonium salts, (b) Raman spectra of biochar and carboxyphenyl-modified biochar using a  $10^{-3}$  M aromatic amine solution, (c) plot of D/G vs mass loading (wt.%) for different biochar samples, and (d) schematic

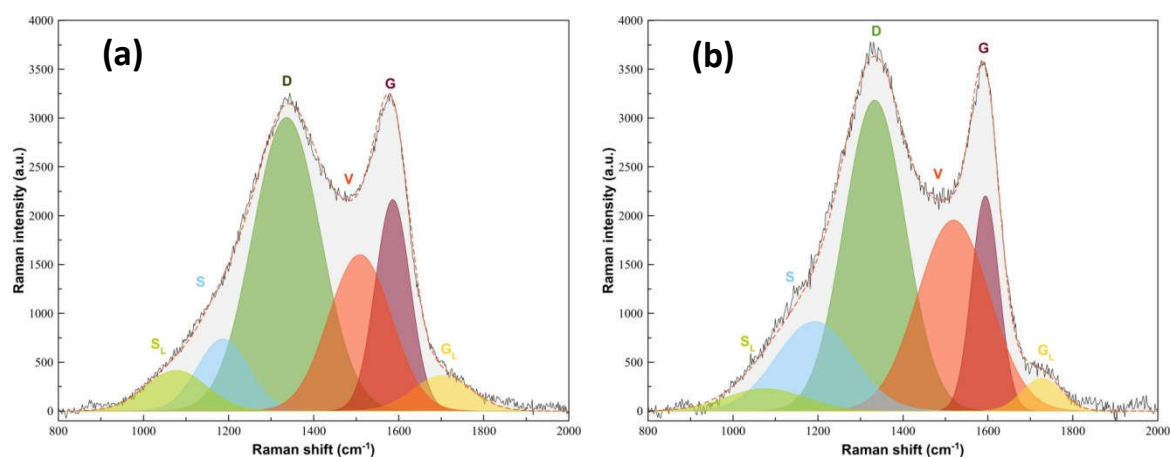


illustration of stepwise growth of oligoaryl chains and their effect on D/G peak area ratio. Reprinted from[65] with the permission of Springer Nature.

Snoussi et al. [68] prepared biochar from the pyrolysis of the pulp of sugarcane pulp bagasse (PSCB) at 500 °C, and modified it with sulfanilic acid-based, in situ generated diazonium salts. AgCu bimetallic nanocatalysts was loaded by in situ reduction of the silver and copper nitrate-impregnated arylated biochar (SO<sub>3</sub>H-Biochar), using phytochemicals extracted from the biomass. Sulfonation and deposition of the bimetallic AgCu nanocatalysts were probed by XPS (Figure 12A). Raman spectra (Figure 12B) curve fitting permitted to determined D and G band area and height. This curve-fitting permitted to show deformations in the carbon lattice resulting from the arylation process with some disorders when compared to the pristine biochar (Figure 12Ba,b). A noticeable increase in biochar defects can be referred to the surface arylation (Figure 12Bb), whereas with a minor effect resulting in slightly higher D/G band intensity ratio. However, upon metal deposition, a significant relative increase in the G band area or height and thus decrease in D/G band area or peak height intensity ratio suggested increase in the graphitization, resulting in boosting the catalytic efficiency.



(B)



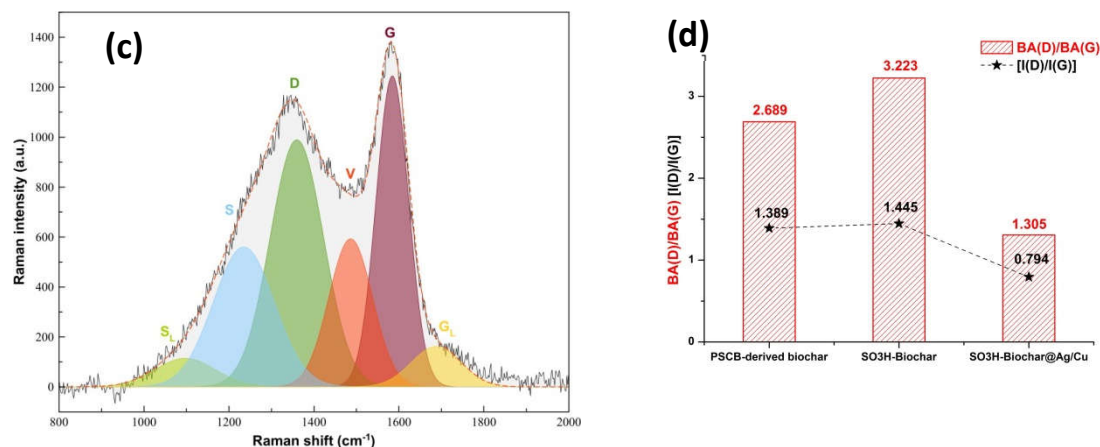


**Figure 12.** Curve fitting of Raman spectra of (a) sugarcane pulp bagasse (PSCB)-derived biochar, (b) SO<sub>3</sub>H-Biochar, (c) SO<sub>3</sub>H-Biochar@Ag/Cu, and (d) the evolution of BA(D)/BA (G) and I(D)/I(G) ratios based on the curve fitting calculations.

Arylation of the activated carbon with 4-sulfo benzene diazonium chloride was carried out for synthesizing 4-sulfophenyl activated carbon to act as an efficient catalyst. Changing the conditions of the reaction provided an arylated activated carbon with sulfanilic acid possessing numerous acid sites. The used catalyst was recovered easily upon utilizing it in esterification reactions of some fatty acids [69]. Bamboo activated carbon was arylated by sulfanilic acid to produce heterogeneous catalysts. The prepared arylated catalysts showed high activity in esterifying oleic acid with alcohol. The microstructure shrinkage may lead to deactivating the heterogeneous acid catalyst. Meanwhile, the regenerated catalyst can be used with providing efficiency over 90% [70]. Sulfonated sucrose-based and N-doped activated carbon were prepared using N-source, pore-forming, and sulfonating agent to act as catalysts. They were then employed in producing furfural from wheat straw (Figure 13). One of these modified catalysts showed acceptable recyclability. The aromatic sulfanilic acid groups were successfully grafted onto the activated carbons via a simple sulfonation procedure [71].

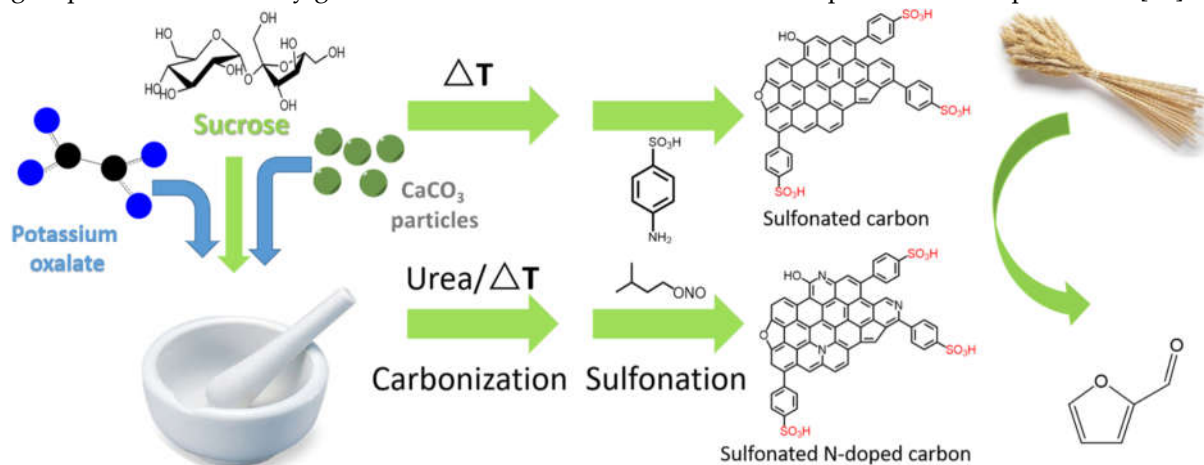


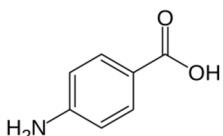
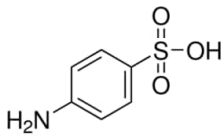
**Figure 13.** Schematic illustration of the preparation of sulfonated biochar as a catalyst of furfural production from wheat straw. Reproduced from [71] with permission of Elsevier.

In another study, sulfonated bio-carbon samples were prepared via partial carbonization of biomass-based substrates with sulfuric acid or diazonium salt. The performance of the catalysts relied upon the concentration of sulfonic acid groups [72]. Sulfonated carbon materials are covalently functionalized with sulfonic acid groups. They show promising efficiency and selectivity, surpassing traditional acid catalysts. The eminent performance of sulfonated carbonaceous substrates may be correlated to their distinctive topographical features, enhancing catalysis and selective adsorption

[73]. Amino-arene-sulfonic acid was used to sulfonate biochar for producing a hydrophobic sulfonic acid functional biochar in a one-pot diazo-reduction process. The length of the arene chain and the grafting magnitude of arenesulfonic acid are substantial factors in monitoring the hydrophobicity of the functionalized biochar catalysts. The latter have a large surface area with an appropriate pore size distribution. This modified biochar supplies an active catalyst in many transformation reactions. These catalysts showed catalytic efficiencies in alkylating 2-methylfuran with cyclopentanone in biofuel production [74].

Table 4 gathers the salient features of some biochar samples arylated under diverse conditions, and for various applications such as the catalysed transformation of furfural, or esterification reaction. Arylation is certainly of interest, but if it is conducted with high initial diazonium concentration, it will lead to sharp decrease of the specific surface area, and the porous volume. Arylation with in situ generated diazonium salts requires strong acidic medium, i.e., 25-37% HCl. This could favours the formation of a porous structure.

**Table 4.** Surface treatment of biochar with aryl diazonium salts.

Coupling agent	Biomass	Surface treatment conditions	Properties of engineered biochar	Potential application	References
	Pomegranate peel	Reaction with in situ generated diazonium salt, in 37% HCl, amine:NaNO <sub>2</sub> = 1:1; final diazonium concentration=10 <sup>-5</sup> -10 <sup>-3</sup> M	Controlled arylation, mass loading = 2.2-10.6 wt/wt%, D/G=2.7-3.4 (peak area ratio).	NA, potential heavy metal removal,	[65]
	Sugarcane bagasse	Reaction of 300 mg biochar with in situ generated diazonium salt, in 37% HCl, amine:NaNO <sub>2</sub> = 1:1 (6 mmol:6 mmol);	Arylation yields the grafting of 2 SO <sub>3</sub> per 100 biochar carbon atoms. D/G=1.39 for biochar and 1.45 for biochar-SO <sub>3</sub> H. Arylation with in situ generated diazonium in concentrated HCl induces channel formation within the biochar.	In situ deposition of Ag(I) and Cu(II) ions, followed by reduction using sugarcane bagasse extract.	[68]
	Pomegranate peel	Reaction with in situ generated diazonium salt, in 37% HCl, amine:NaNO <sub>2</sub> = 1:1; final diazonium concentration=10 <sup>-3</sup> M	Mass loading = 5.3%, D/G=2.9 (peak area ratio)	NA, potential heavy metal removal	[65]
	Bamboo	Sulfanilic acid/Biochar molar ratio= 0.1-1.5, in 25% HCl, at 30-80 °C, for 2-60 min.	Total acid density=1.69 mmol/g. SSA decreased from 919 to 225 m <sup>2</sup> /g upon arylation.	Acid catalyst. Up to 96% catalyzed esterification of oleic acid with ethanol.	[70]
	Sucrose-K <sub>2</sub> C <sub>2</sub> O <sub>4</sub> •H <sub>2</sub> O-CaCO <sub>3</sub> -Urea (1-1-1-0 or 1-1-1-0.5 wt.fractions)	Biochar prepared at 600-800 °C without urea, and at 750 °C in the presence of urea. 1g biochar mixed with 4 g sulfanilic acid and 2 g isoamyl nitrite, in 150 mL DIW. Arylation at 80 °C overnight.	Drastic reduction of SSA from 1422 to 190 m <sup>2</sup> /g for biochar prepared at 800 °C, and from 1658 to 30 m <sup>2</sup> for biochar-urea and sulfonated biochar-urea. Sulfur content: 0.08 to 2.29 mmol/g. With urea, very high arylationD/G increased with arylation.	Catalytic furfural production from wheat straw.	[71]

 $\text{Cl}^-$	Pomegranate peel	Reaction with in situ generated diazonium salt, in 37% HCl, amine: $\text{NaNO}_2 = 1:1$ ; final diazonium concentration= $10^{-3}$ M	Mass loading = 5.3%, D/G=2.9 (peak area ratio)	NA, potential radical polymerization photoinitiation	[65]
-------------------	------------------	--	---	--	------

APTES: aminopropyl triethoxysilane; DIW: de-ionized water; SSA: specific surface area.

## 2.6. Surface-Modified Biochar with Nitrogen-Based Compounds

Owing to the versatility of  $\text{sp}^2$  carbon surface, and the availability of highly interacting functional groups, biochar is prone to molecular and macromolecular post-functionalization with aminated compounds. Doping biochar with nitrogen-containing compounds during pyrolysis or hydrothermal treatment of the biomass is out of scope and the reader is referred to selected articles on the topic [75–77]. Similarly, strong activation with nitric acid to provide surface amino groups is covered but not with dedicated section; as an example see for example the work of Bamdad *et al.* [78]

Modification can proceed with molecular coupling agent, or with adsorption of a monomer that is subjected to polymerization.

Two major nitrogen-containing compounds have been employed to modify the surface of biochar: aniline and 2-aminothiophenol related compounds, and polyethyleneimine (PEI). The aniline derivatives are usually subjected to in situ oxidative polymerization in the presence of biochar. Surface confined polymerization proceeds with adsorption of the aniline derivative, most probably driven by biochar-COOH... $\text{H}_2\text{N}-\text{C}_6\text{H}_4-\text{R}$  hydrogen bonding. For example 2-aminothiophenol can be adsorbed on the surface of biochar and subjected to oxidative polymerization using ammonium persulfate to yield poly(2-aminothiophenol)-coated biochar particles (Figure 14) [79]. Note that, in Figure 14, hydrogen bonds are shown for N...N interactions; in our fair opinion hydrogen bonds occur between  $\text{NH}_2$  from the monomer and the COOH and/or OH from the biochar surface. Indeed, Lewis acid-base interactions, or more particularly hydrogen bonds are maximized for COOH- $\text{NH}_2$  rather than  $\text{NH}_2-\text{NH}_2$  interactions [80]. The biochar composite was tested for the uptake of Hg and As from wastewater and was found to remove over twice as much contaminants, at pH 9, compared to the untreated biochar. Adsorption levelled off at ~32 and 119 mg/g As(III) and Pb(II), respectively. These values are much higher than those recorded with unmodified biochar (14 and 47 mg/g for AS(III) and Pb(II), respectively). At this stage, it is essential to note that despite drastic two-fold decrease of the specific surface area of the engineered biochar owing to the polymer coating (118 and 59  $\text{m}^2/\text{g}$  for engineered and pristine biochar, respectively), removal of As(III) and Pb(II) remained high.

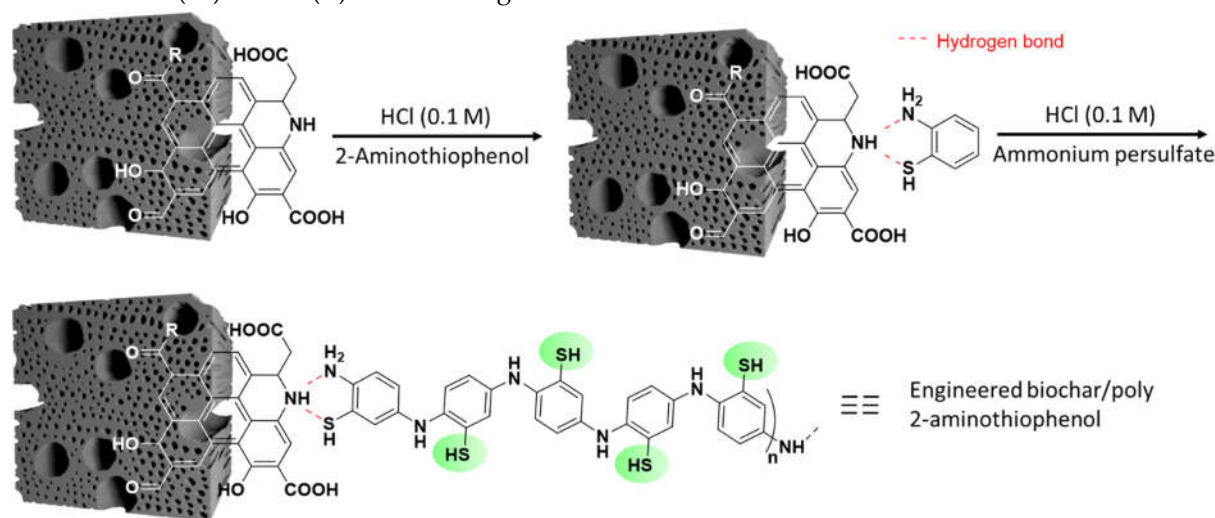


**Figure 14.** Schematic illustration of the route to engineered biochar/poly(2-aminothiophenol) adsorbent via in situ oxidative polymerization of 2-aminothiophenol. Reproduced from [79] with permission of Elsevier.

Aniline is a much more investigated monomer to provide composites of biochar and polyaniline (PANI). It can be synthesized in the presence of biochar and remains glued to biochar via hydrogen bonds (Figure 15).

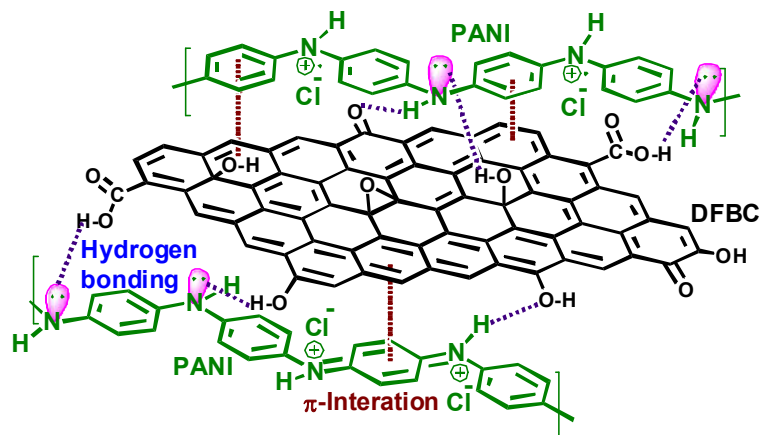


**Figure 15.** Biochar-PANI composite chemical structure. Dotted lines indicate hydrogen and p-p bonds between biochar and the PANI deposit. Reproduced from [81] with permission of Elsevier.

Douglas fir biochar was prepared by fast pyrolysis at 900-1000 °C, and served for the in situ deposition of PANI by oxidative polymerization [81]. 1g biochar-PANI composite removed 150 mg Cr(VI) and 72 mg nitrates, at pH 2 and 6, respectively, much more than the pristine biochar. PANI provides nitrogen-based anchoring sites for Cr(VI) and hydrogen bonding acceptor from biochar OH and COOH groups.

Magnetic biochar-PANI composites were prepared by wet impregnation of durian rinds powder with three iron precursor, followed by pyrolysis at 800 °C. The resulting magnetic biochars were further coated with PANI via in situ oxidative polymerization of aniline using ammonium persulfate, in acidic medium (1 M HCl), at 0-5 °C. The highest specific surface was 855 m<sup>2</sup>/g. The magnetic biochar prepared using FeCl<sub>3</sub>·6H<sub>2</sub>O precursor and topped with PANI was used as supercapacitor; it exhibited a specific capacitance of 615 F/g at 10 mV/s and energy density of 76.9 Wh/kg [82].

Magnetic banana stem biochar was prepared in situ deposition of magnetite after the carbonization process of the biomass at 500 °C. PANI was prepared by in situ polymerization to yield a supercapacitor composite material that has a specific capacitance  $C_s = 315.7 \text{ Fg}^{-1}$ , higher than that of the magnetic biochar without any PANI ( $C_s = 234.8 \text{ Fg}^{-1}$ ) [83].

Tobacco biochar was fabricated, treated with phosphoric acid and mixed with PANI, then Ag<sub>3</sub>PO<sub>4</sub> was synthesized in situ. The final Biochar/PANI/Ag<sub>3</sub>PO<sub>4</sub> was employed as photocatalyst to degrade triclosan [84]. The rationale for making this ternary composite lies in the synergy between (i) the excellent photocatalytic properties of Ag<sub>3</sub>PO<sub>4</sub>, (ii) the electronic conductivity of biochar that favours rapid transfer of photogenerated electron (e<sup>-</sup>) of Ag<sub>3</sub>PO<sub>4</sub>, and (iii) PANI, a promoter of the transfer and separation of photogenerated hole-electron pairs (h<sup>+</sup>-e<sup>-</sup>), as well as an inhibitor of the photo-corrosion and oxidation of Ag<sub>3</sub>PO<sub>4</sub>. The composite catalysed the degradation of triclosan at a rate of 85%, within 10 min.

Another type of biochar/polymer composites can be prepared by mixing biochar with PEI, using methanol or ethanol.[85–89] Electrostatic interaction between the protonated amino groups from the biochar and the carboxylate groups from biochar can take place. Also, strong hydrogen bonds are expected. Covalent grafting of PEI could be achieved using glutaraldehyde [23,90] or EDTA dianhydride [86]. For example, the frequently employed glutaraldehyde is a good coupling agent as it reacts with OH functional groups [91] from biochar surface and the NH/NH<sub>2</sub> groups from PEI. An example of composite is illustrated in Figure 16 showing the fabrication of magnetic biochar-PEI nanocomposite employed for the removal of Cr(VI).



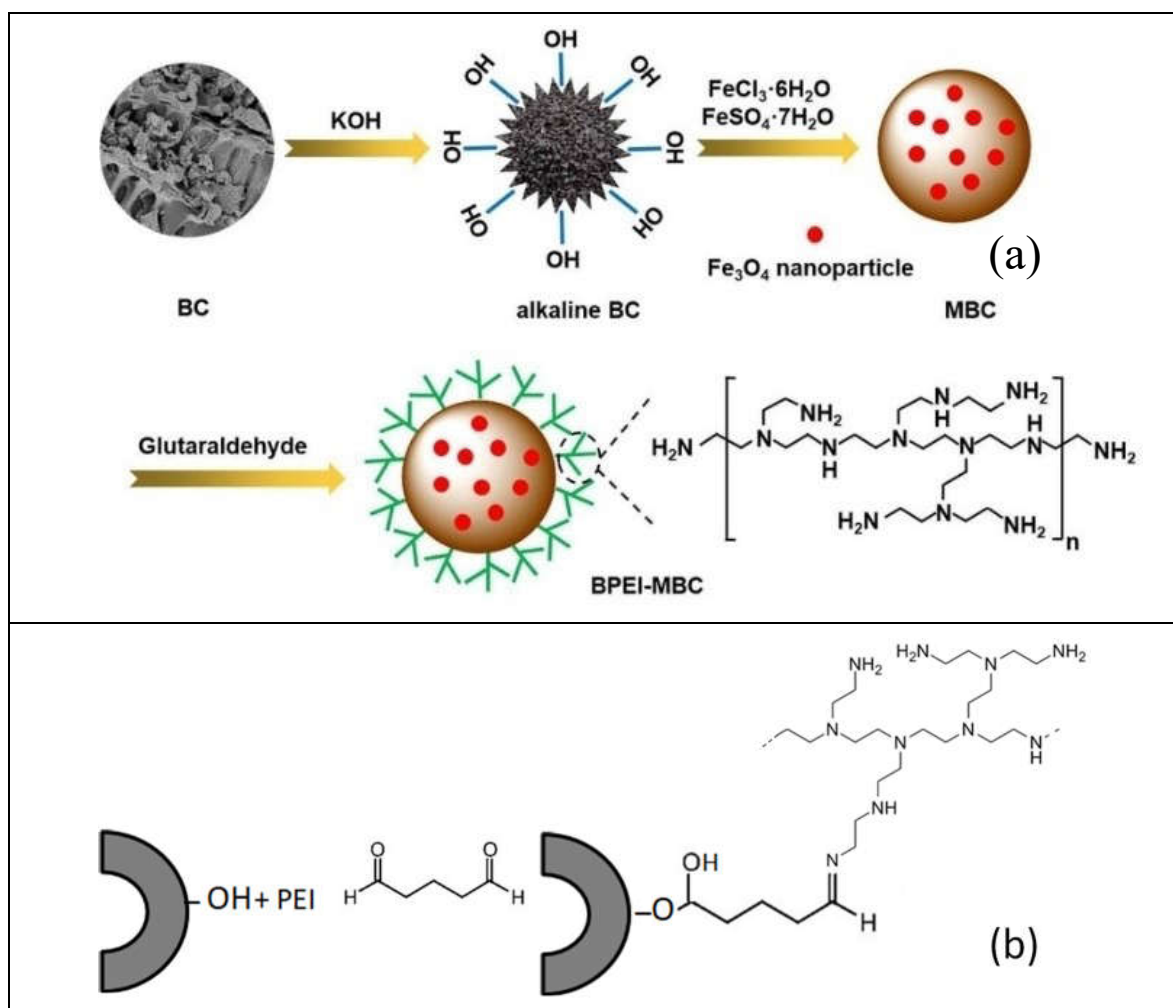


**Figure 16.** Schematic illustration of the fabrication of magnetic coconut shell biochar and its graft modification with PEI (a). Use of glutaraldehyde for coupling PEI to the underlying biochar (b). Figure 16a reproduced from with permission of Wiley & Sons.

As a few examples of the performance of PEI-modified biochar materials, PEI-modified pine needles biochar permitted to adsorb 294 mg/g Congo Red, almost 10-fold the adsorption capacity of the pristine biochar (30.8 mg/g) [92].

PEI-modified biochar was employed for detoxification of Cr(VI); it was found to remove 435.7 mg per g biochar, nearly 20 times higher than 23.1 mg/g for pristine biochar [85].

### 3. Conclusions

In this review, we have summarized the essential findings on the molecular and macromolecular level of biochar surface treatment. We have covered the modifications of numerous biochar types with silane and titanate coupling agents, aryl diazonium salts, ionic and non-ionic surfactants, and nitrogen-containing compounds. The latter could be a polymerizable monomer (aniline derivatives) or a preformed polymer such as polyethylenimine (PEI) adsorbed from an alcoholic solution.

One could draw numerous conclusions:

- in general, surface modification reduces the specific surface area and porous volume, but it is worth it because it imparts functionalities that unmodified biochar samples do not possess
- silanization requires rich oxygen functionalities at the surface which could be obtained at moderate pyrolysis temperature, or after oxidization of the biochar.
- titanate could be envisaged to create new biochar-polymer composites, if the primary intention is not to design biochar-titania photocatalysts

- aryl diazonium could be regarded as new coupling agents in materials surface chemistry as witnessed over the last three decades; their use to modify biochar particles is recent and very encouraging. Some of us have demonstrated that surface modification is limited by steric hindrance effects of the aryl group, and change in carbon structure of the biochar is significant at low initial diazonium concentration
- modification with non-ionic and ionic surfactant adsorbed layers influences the textural characteristics of biochar, as well as acido-basic and hydrophilic-hydrophobic properties of its surface, changing the affinity for other substances present in the aqueous phase. The electrostatic, hydrogen bonds,  $\pi$ - $\pi$  electrons and hydrophobic interactions are responsible for the surfactant molecules binding and can result in the formation of more complex surface structures, such as surfactant-adsorbate multilayers and micelles.
- the preparation of biochar-polyaniline composites are investigated by several researchers, particularly for the fabrication of supercapacitors, whereas poly(2-aminothiophenol) could be a remarkable alternative to provide surface-immobilized NH and SH groups able to chelate metal ions, for environmental remediation issues
- polyethyleneimine is a nitrogen-rich polymer, and could be coated on biochar particles by adsorption from methanol or ethanol solution. Tight, covalent immobilization and crosslinking requires using organic coupling agents such as glutaraldehyde.

These are the most investigated surface modifiers but others are worth deeper insight, *e.g.* mercaptoethanol [93] and vitamin-B6. [94]. Nevertheless, all in one, there is much to anticipate from surface chemical modification of biochar in the coming years. Surface modification imparts remarkable new functionalities such as pollutant adsorption, immobilization of catalysts, improved energy storage properties, to name but a few.

Concerning bulk, surface and textural properties, we witnessed recurrent utilization of XPS, Raman and FTIR, XRD, nitrogen adsorption (for BET and porous volume), and TGA. Other techniques are also applied in the case of specific applications such as energy storage, namely DC voltage-current measurements, and cyclic voltammetry. Ironically, we have noted that the biochar topic tackles the valorization of wastes, with zero value, but requires a high number of analytical techniques, which is excessively costly for academic laboratories.

From the above, the conversion of agro- and other organic wastes into biochar is a very hot topic with over 5500 publications a year. This will continue to grow in this era of economic crisis, on the one hand, and to address some of 17 sustainable development goals, on the other hand. We thus expect even more publications on the topic and the valorization of numerous other wastes. There are already, and there will be new regional niches from North to South to valorize biomasses such as Douglas fir, [81] brewer spent grain, [95] sugarcane bagasse, [68] olive [96,97] and date [98] stones, durian, [82]. However, more rationality is needed to select which agrowaste is worth the thermochemical transformation into biochar, by determining the initial cellulose-hemicellulose-lignin composition as their thermochemical transformation yields biochars with completely different properties and thus different potential applications, for example as electrode materials [10]. Pyrolysis is interesting and offers advantages, but for other applications, hydrochars could be a solution because the treatment is faster, and the process might provide extraction of phytochemical useful for reductive reaction processes, [12] and also carbon dots [99]. Recently, microwave heating has emerged as an alternative for the fabrication of carbonaceous chars, with low energy cost of preparation, and remarkable properties [98]. Yet, when it comes to surface modification, this review has indicated numerous opportunities, but also challenges to overcome, such as the balance between surface chemistry and textural properties in order to achieve the desired end properties and performances.

**Authors' contributions:** Conceptualization (AMK, MW, MMC); Methodology (MMC, MW); Validation (all authors); Writing-Original Draft (AMK, MW, MMC); Writing - Review & Editing (all authors); Resources (MMC, AMK, MW); Supervision (MMC); Funding acquisition (AMK, MMC, AKB, YS).

**Funding:** MK and MMC would like to thank both the French Government for funding AMK's contribution through a fellowship granted by the French Embassy in Egypt (Institut Francais d'Egypte). AKB thanks WBI for the provision of a grant "Bourse Wallonie-Bruxelles International Excellence World (N° imputation – 101386, and Article Budgétaire – 33.01.00.07)".

**Institutional Review Board Statement:** Not applicable.

**Informed Consent Statement:** Not applicable.

**Data Availability Statement:** Not applicable.

**Conflicts of Interest:** the authors declare no conflict of interest.

## References

1. S. Adhikari, W. Timms, M. A. P. Mahmud, *Sci. Total Environ.* **2022**, *851*, 158043 <https://doi.org/10.1016/j.scitotenv.2022.158043>.
2. S. Wijitkosum, *Int. Soil Water Conserv. Res.* **2022**, *10*, 335–341 <https://doi.org/10.1016/j.iswcr.2021.09.006>.
3. M. Harussani, S. Sapuan, *Chem. Afr.* **2021**, 1–17.
4. H. Liu, Y. Liu, X. Li, X. Zheng, X. Feng, A. Yu, in *Book Adsorption and Fenton-like Degradation of Ciprofloxacin Using Corncob Biochar-Based Magnetic Iron&ndash;Copper Bimetallic Nanomaterial in Aqueous Solutions*, ed., ed. by Editor, City, **2022**, Volume 12, Chap. Chapter.
5. A. Mukherjee, N. Goswami, D. Dhak, *Chem. Afr.* **2022**. <https://doi.org/10.1007/s42250-022-00467-5>.
6. M. Bartoli, R. Arrigo, G. Malucelli, A. Tagliaferro, D. Duraccio, *Polymers* **2022**, *14*, 2506.
7. N. Bélanger, S. Prasher, M.-J. Dumont, *Polym. -Plast. Technol. Mater.* **2023**, *62*, 54–75 <https://doi.org/10.1080/25740881.2022.2089584>.
8. M. M. Harussani, S. M. Sapuan, G. Nadeem, T. Rafin, W. Kirubaanand, *Def. Technol.* **2022**, *18*, 1281–1300 <https://doi.org/10.1016/j.dt.2022.03.006>.
9. T. Huggins, H. Wang, J. Kearns, P. Jenkins, Z. J. Ren, *Bioresour. Technol.* **2014**, *157*, 114–119.
10. S. Tabac, D. Eisenberg, *Curr. Opin. Electrochem.* **2021**, *25*, 100638 <https://doi.org/10.1016/j.coelec.2020.09.005>.
11. Y. Snoussi, I. Sifaoui, A. M. Khalil, A. K. Bhakta, O. Semyonov, P. S. Postnikov, L. Michely, R. Pires, S. Bastide, J. E.-P. Barroso, J. L. Morales, M. M. Chehimi, *Mater. Today Commun.* **2022**, *32*, 104126 <https://doi.org/10.1016/j.mtcomm.2022.104126>.
12. Y. Snoussi, I. Sifaoui, M. El Garah, A. M. Khalil, J. E. Piñero, M. Jouini, S. Ammar, J. Lorenzo-Morales, M. M. Chehimi, *Waste Manag.* **2023**, *155*, 179–191 <https://doi.org/10.1016/j.wasman.2022.11.006>.
13. H. W. Lee, H. Lee, Y.-M. Kim, R.-s. Park, Y.-K. Park, *Chin. Chem. Lett.* **2019**, *30*, 2147–2150 <https://doi.org/10.1016/j.ccl.2019.05.002>.
14. U. Kamran, S.-J. Park, *J. Clean. Prod.* **2021**, *290*, 125776 <https://doi.org/10.1016/j.jclepro.2020.125776>.
15. R. P. Lopes, D. Astruc, *Coord. Chem. Rev.* **2021**, *426*, 213585.
16. D. Luo, L. Wang, H. Nan, Y. Cao, H. Wang, T. V. Kumar, C. Wang, *Environ. Chem. Lett.* **2022**. <https://doi.org/10.1007/s10311-022-01519-5>.
17. L. Goswami, A. Kushwaha, S. R. Kafle, B.-S. Kim, *Catalysts* **2022**, *12*, 817.
18. D. C. C. d. S. Medeiros, C. Nzediegwu, C. Benally, S. A. Messele, J.-H. Kwak, M. A. Naeth, Y. S. Ok, S. X. Chang, M. Gamal El-Din, *Sci. Total Environ.* **2022**, *809*, 151120 <https://doi.org/10.1016/j.scitotenv.2021.151120>.
19. X. Pan, Z. Gu, W. Chen, Q. Li, *Sci. Total Environ.* **2021**, *754*, 142104.
20. M. M. Chehimi, J. Pinson, F. Mousli, *Aryl Diazonium Salts and Related Compounds: Surface Chemistry and Applications*. Editor, Springer Nature, **2022**.
21. C. Li, Y. Gao, A. Li, L. Zhang, G. Ji, K. Zhu, X. Wang, Y. Zhang, *Environ. Pollut.* **2019**, *254*, 113005 <https://doi.org/10.1016/j.envpol.2019.113005>.
22. F. Asgharzadeh, R. R. Kalantary, M. Gholami, A. J. Jafari, M. Kermani, H. Asgharnia, *Biomass Convers. Biorefinery* **2021**. <https://doi.org/10.1007/s13399-021-01685-6>.
23. X. Wang, J. Feng, Y. Cai, M. Fang, M. Kong, A. Alsaedi, T. Hayat, X. Tan, *Sci. Total Environ.* **2020**, *708*, 134575 <https://doi.org/10.1016/j.scitotenv.2019.134575>.
24. S. Detriche, A. K. Bhakta, P. N'Twali, J. Delhalle, Z. Mekhalif, in *Book Assessment of Catalyst Selectivity in Carbon-Nanotube Silylation*, ed., ed. by Editor, City, **2020**, Vol. 10, Chap. Chapter.
25. P. Walker, *Handbook of adhesive technology* **2003**, *2*, 205–221.
26. Y. Lan, W. Wang, *Adv. Polym. Technol.* **2018**, *37*, 1979–1986 <https://doi.org/10.1002/adv.21856>.
27. M. Zhang, H. Zhu, B. Xi, Y. Tian, X. Sun, H. Zhang, B. Wu, in *Book Surface Hydrophobic Modification of Biochar by Silane Coupling Agent KH-570*, ed., ed. by Editor, City, **2022**, Vol. 10, Chap. Chapter.

28. H. Bamdad, K. Hawboldt, S. MacQuarrie, *Energy Fuels* **2018**, 32, 11742–11748 [10.1021/acs.energyfuels.8b03056](https://doi.org/10.1021/acs.energyfuels.8b03056).
29. P. Moradi, M. Hajjami, *RSC Adv.* **2022**, 12, 13523–13534 [10.1039/D1RA09350A](https://doi.org/10.1039/D1RA09350A).
30. P. Moradi, M. Hajjami, *New J. Chem.* **2021**, 45, 2981–2994.
31. Y. Huang, S. Xia, J. Lyu, J. Tang, *Chem. Eng. J.* **2019**, 360, 1646–1655 <https://doi.org/10.1016/j.cej.2018.10.231>.
32. W. Ran, H. Zhu, X. Shen, Y. Zhang, *Constr. Build. Mater.* **2022**, 329, 127057 <https://doi.org/10.1016/j.conbuildmat.2022.127057>.
33. B. Wu, B. Xi, X. He, X. Sun, Q. Li, Q. Oucho, H. Zhang, C. Xue, in *Book Methane Emission Reduction Enhanced by Hydrophobic Biochar-Modified Soil Cover*, ed., ed. by Editor, City, **2020**, Vol. 8, Chap. Chapter.
34. K. Sheng, S. Zhang, S. Qian, C. A. Fontanillo Lopez, *Compos. Part B: Eng.* **2019**, 165, 174–182 <https://doi.org/10.1016/j.compositesb.2018.11.139>.
35. Y. Qin, B. Xi, X. Sun, H. Zhang, C. Xue, B. Wu, *Front. Bioeng. Biotechnol.* **2022**, 10, <https://doi.org/10.3389/fbioe.2022.905466>.
36. G. Devi, N. Nagabhooshanam, M. Chokkalingam, S. K. Sahu, *Polym. Compos.* **2022**, 43, 5996–6003 <https://doi.org/10.1002/pc.26898>.
37. P. Moradi, M. Hajjami, F. Valizadeh-Kakhki, *Appl. Organomet. Chem.* **2019**, 33, e5205 <https://doi.org/10.1002/aoc.5205>.
38. H. Li, L. Sun, W. Li, *J. Mater. Sci.* **2022**, 57, 13845–13870 [10.1007/s10853-022-07488-y](https://doi.org/10.1007/s10853-022-07488-y).
39. Y. Lu, X. Li, C. Wu, S. Xu, *J. Alloys Compd.* **2018**, 750, 197–205 <https://doi.org/10.1016/j.jallcom.2018.03.301>.
40. N. W. Elshereksi, M. Ghazali, A. Muchtar, C. H. Azhari, *Dent. Mater. J.* **2017**, 2016–014.
41. B. Ali Sabri, S. Meenaloshini, N. M. Abreeza, A. N. Abed, *Mater. Today: Proc.* **2021**, <https://doi.org/10.1016/j.matpr.2021.06.340>.
42. Y. Zeng, Y. Xue, L. Long, J. Yan, *Water Air Soil Pollut.* **2019**, 230, 50 [10.1007/s11270-019-4104-2](https://doi.org/10.1007/s11270-019-4104-2).
43. K. D. Cai, W. F. Mu, in *Book Activated carbon modified by titanate coupling agent for supercapacitor*, ed., ed. by Editor, Trans Tech Publ, City, **2012**, Vol. 347, Chap. Chapter, pp. 3649–3652.
44. X. Li, C. Gan, Z. Han, H. Yan, D. Chen, W. Li, H. Li, X. Fan, D. Li, M. Zhu, *Carbon* **2020**, 165, 238–250 <https://doi.org/10.1016/j.carbon.2020.04.038>.
45. M. Shahverdi, E. Kouhgard, B. Ramavandi, *Data Brief* **2016**, 9, 163–168 <https://doi.org/10.1016/j.dib.2016.08.051>.
46. L. Mathurasa, S. Damrongsiri, *Appl. Environ. Res.* **2017**, 39, 11–22.
47. M. Wiśniewska, P. Nowicki, T. Urban, *J. Mol. Liq.* **2021**, 332, 115872 <https://doi.org/10.1016/j.molliq.2021.115872>.
48. F. Wang, Q. Zeng, W. Su, M. Zhang, L. Hou, Z.-L. Wang, *J. Chem.* **2019**, 2019, 2428505. <https://doi.org/10.1155/2019/2428505>.
49. C. Kosaiyakanon, S. Kungsanant, *Environ. Nat. Resour. J.* **2019**, 18, 21–32.
50. X. Mi, G. Li, W. Zhu, L. Liu, *J. Chem.* **2016**, 2016.
51. M. Wiśniewska, P. Nowicki, *Colloids Surf. A: Physicochem. Eng. Asp.* **2020**, 585, 124179 <https://doi.org/10.1016/j.colsurfa.2019.124179>.
52. A. K. Anas, S. Y. Pratama, A. Izzah, M. A. Kurniawan, *2021* **2021**, 8, <https://doi.org/10.9767/bcrec.16.1.10323.188-195>.
53. A. K. Anas, A. Izzah, S. Y. Pratama, F. I. Fajarwati, *AIP Conf. Proc.* **2020**, 2229, 030024. <https://doi.org/10.1063/5.0002675>.
54. W. Que, L. Jiang, C. Wang, Y. Liu, Z. Zeng, X. Wang, Q. Ning, S. Liu, P. Zhang, S. Liu, *J. Environ. Sci.* **2018**, 70, 166–174. <https://doi.org/10.1016/j.jes.2017.11.027>.
55. H. He, W. Li, H. Deng, L. Kang, R. Qiu, X. Li, W. Liu, Z. Meng, *Desalination Water Treat.* **2019**, 148, 195–201.
56. M. Wiśniewska, P. Nowicki, K. Szewczuk-Karpisz, M. Gęca, K. Jędruchiewicz, P. Oleszczuk, *Sep. Purif. Technol.* **2021**, 276, 119297. <https://doi.org/10.1016/j.seppur.2021.119297>.
57. Z. Hua, S. Wan, L. Sun, Z. Yu, X. Bai, *J. Chem. Technol. Biotechnol.* **2018**, 93, 3044–3055 <https://doi.org/10.1002/jctb.5663>.
58. P. Griess, *Annalen* **1858**, 106, 123–125.
59. S. V. Heines, *J. Chem. Educ.* **1958**, 35, 187. <https://doi.org/10.1021/ed035p187>.
60. F. Mo, G. Dong, Y. Zhang, J. Wang, *Org. Biomol. Chem.* **2013**, 11, 1582–1593. <https://doi.org/10.1039/C3OB27366K>.
61. A. A. Mohamed, Z. Salmi, S. A. Dahoumane, A. Mekki, B. Carbonnier, M. M. Chehimi, *Adv. Colloid Interface Sci.* **2015**, 225, 16–36.
62. P. Mirzaei, S. Bastide, A. Aghajani, J. Bourgon, E. Leroy, J. Zhang, Y. Snoussi, A. Bensghaier, O. Hamouma, M. M. Chehimi, *Langmuir* **2019**, 35, 14428–14436.
63. A. S. A. Ali H. Jawad, Lee D. Wilson, Syed Shatir A. Syed-Hassan, Zeid A. AlOthman, Mohammad Rizwan Khan, *Chin. J. Chem. Eng.* **2021**, 32, 281–290. <https://doi.org/10.1016/j.cjche.2020.09.070>.
64. M. H. Abdel-Aziz, E. Z. El-Ashtoukhy, M. Bassyouni, A. F. Al-Hossainy, E. M. Fawzy, S. M. S. Abdel-Hamid, M. S. Zoromba, *Carbon Lett.* **2021**, 31, 863–878. <https://doi.org/10.1007/s42823-020-00187-1>.



65. A. M. Khalil, R. Msaadi, W. Sassi, I. Ghanmi, R. Pires, L. Michely, Y. Snoussi, A. Chevillot-Biraud, S. Lau-Truong, M. M. Chehimi, *Carbon Lett.* **2022**, 32, 1519–1529. <https://doi.org/10.1007/s42823-022-00374-2>.
66. A. L. Rodd, M. A. Creighton, C. A. Vaslet, J. R. Rangel-Mendez, R. H. Hurt, A. B. Kane, *Environ. Sci. Technol.* **2014**, 48, 6419–6427. <https://doi.org/10.1021/es500892m>.
67. A. Bensghaïer, Z. Salmi, B. Le Droumaguet, A. Mekki, A. A. Mohamed, M. Beji, M. M. Chehimi, *Surf. Interface Anal.* **2016**, 48, 509–513.
68. Y. Snoussi, M. El Garah, A. M. Khalil, S. Ammar, M. M. Chehimi, *Appl. Organomet. Chem.* **2022**, 36, e6885 <https://doi.org/10.1002/aoc.6885>.
69. K. Malins, V. Kampars, J. Brinks, I. Neibolte, R. Murnieks, *Appl. Catal. B: Environ.* **2015**, 176–177, 553–558 <https://doi.org/10.1016/j.apcatb.2015.04.043>.
70. S. Niu, Y. Ning, C. Lu, K. Han, H. Yu, Y. Zhou, *Energy Convers. Manag.* **2018**, 163, 59–65 <https://doi.org/10.1016/j.enconman.2018.02.055>.
71. T. Zhang, H. Wei, J. Gao, S. Chen, Y. Jin, C. Deng, S. Wu, H. Xiao, W. Li, *Mol. Catal.* **2022**, 517, 112034 <https://doi.org/10.1016/j.mcat.2021.112034>.
72. A. Malaika, K. Ptasińska, M. Kozłowski, *Fuel* **2021**, 288, 119609. <https://doi.org/10.1016/j.fuel.2020.119609>.
73. L. J. Konwar, P. Mäki-Arvela, J.-P. Mikkola, *Chem. Rev.* **2019**, 119, 11576–11630. <https://doi.org/10.1021/acs.chemrev.9b00199>.
74. Y. Zhong, Q. Deng, P. Zhang, J. Wang, R. Wang, Z. Zeng, S. Deng, *Fuel* **2019**, 240, 270–277 <https://doi.org/10.1016/j.fuel.2018.11.152>.
75. Z. Wan, Y. Sun, D. C. W. Tsang, E. Khan, A. C. K. Yip, Y. H. Ng, J. Rinklebe, Y. S. Ok, *Chem. Eng. J.* **2020**, 401, 126136 <https://doi.org/10.1016/j.cej.2020.126136>.
76. N. Kaser, P. Kolar, S. G. Hall, *Biochar* **2022**, 4, 17 <https://doi.org/10.1007/s42773-022-00145-2>.
77. Z. Lin, R. Wang, S. Tan, K. Zhang, Q. Yin, Z. Zhao, P. Gao, *J. Environ. Manag.* **2023**, 334, 117503 <https://doi.org/10.1016/j.jenvman.2023.117503>.
78. R. Chatterjee, B. Sajjadi, W.-Y. Chen, D. L. Mattern, N. O. Egiebor, N. Hammer, V. Raman, *Energy Fuels* **2019**, 33, 2366–2380. <https://doi.org/10.1021/acs.energyfuels.8b03583>.
79. M. Shahabi Nejad, H. Sheibani, *J. Environ. Chem. Eng.* **2022**, 10, 107363 <https://doi.org/10.1016/j.jece.2022.107363>.
80. R. C. Thomas, J. E. Houston, R. M. Crooks, T. Kim, T. A. Michalske, *J. Am. Chem. Soc.* **1995**, 117, 3830–3834. <https://doi.org/10.1021/ja00118a019>.
81. A. Herath, C. Reid, F. Perez, C. U. Pittman, T. E. Mlsna, *J. Environ. Manag.* **2021**, 296, 113186 <https://doi.org/10.1016/j.jenvman.2021.113186>.
82. K. R. Thines, E. C. Abdullah, M. Ruthiraan, N. M. Mubarak, M. Tripathi, *J. Anal. Appl. Pyrolysis* **2016**, 121, 240–257 <https://doi.org/10.1016/j.jaap.2016.08.004>.
83. D. Thomas, N. B. Fernandez, M. D. Mullassery, R. Surya, *Inorg. Chem. Commun.* **2020**, 119, 108097 <https://doi.org/10.1016/j.inoche.2020.108097>.
84. Y. Ma, T. Zhang, P. Zhu, H. Cai, Y. Jin, K. Gao, J. Li, *Sci. Total Environ.* **2022**, 821, 153453 <https://doi.org/10.1016/j.scitotenv.2022.153453>.
85. Y. Ma, W.-J. Liu, N. Zhang, Y.-S. Li, H. Jiang, G.-P. Sheng, *Bioresour. Technol.* **2014**, 169, 403–408 <https://doi.org/10.1016/j.biortech.2014.07.014>.
86. J. Qu, X. Zhang, F. Bi, S. Wang, X. Zhang, Y. Tao, Y. Wang, Z. Jiang, Y. Zhang, *Environ. Pollut.* **2022**, 313, 120103 <https://doi.org/10.1016/j.envpol.2022.120103>.
87. M. Geça, M. Wiśniewska, P. Nowicki, in Book Simultaneous Removal of Polymers with Different Ionic Character from Their Mixed Solutions Using Herb-Based Biochars and Activated Carbons, ed., ed. by Editor, City, **2022**, Vol. 27, Chap. Chapter.
88. E. Parameswari, R. Kalaiarasi, V. Davamani, T. Ilakiya, P. Kalaiselvi, S. P. Sebastian, in *Biochar and its Application in Bioremediation*, ed. by R. Thapar Kapoor, H. Treichel, M. P. Shah, Springer Nature Singapore, Singapore, **2021**, pp. 27–48.
89. H. Tian, C. Huang, P. Wang, J. Wei, X. Li, R. Zhang, D. Ling, C. Feng, H. Liu, M. Wang, Z. Liu, *Bioresour. Technol.* **2023**, 369, 128452 <https://doi.org/10.1016/j.biortech.2022.128452>.
90. Q. Jiang, W. Xie, S. Han, Y. Wang, Y. Zhang, *Colloids Surf. A: Physicochem. Eng. Asp.* **2019**, 583, 123962 <https://doi.org/10.1016/j.colsurfa.2019.123962>.
91. Z. Xiao, Y. Xie, H. Militz, C. Mai, **2010**, 64, 483–488. <https://doi.org/10.1515/hf.2010.087>.
92. D. Pandey, A. Daverey, K. Dutta, K. Arunachalam, *Environ. Monit. Assess.* **2022**, 194, 880 <https://doi.org/10.1007/s10661-022-10563-1>.
93. J. Fan, C. Cai, H. Chi, B. J. Reid, F. Coulon, Y. Zhang, Y. Hou, *J. Hazard. Mater.* **2020**, 388, 122037 <https://doi.org/10.1016/j.jhazmat.2020.122037>.
94. F. Saremi, M. R. Miroliaei, M. Shahabi Nejad, H. Sheibani, *J. Mol. Liq.* **2020**, 318, 114126 <https://doi.org/10.1016/j.molliq.2020.114126>.
95. L. Boubkr, A. K. Bhakta, Y. Snoussi, C. Moreira Da Silva, L. Michely, M. Jouini, S. Ammar, M. M. Chehimi, in Book Highly Active Ag-Cu Nanocrystal Catalyst-Coated Brewer’s Spent Grain Biochar for the



Mineralization of Methyl Orange and Methylene Blue Dye Mixture, ed., ed. by Editor, City, **2022**, Vol. 12, Chap. Chapter.

96. J. Omiri, Y. Snoussi, A. K. Bhakta, S. Truong, S. Ammar, A. M. Khalil, M. Jouini, M. M. Chehimi, *Colloids Interfaces* **2022**, 6. <https://doi.org/10.3390/colloids6020018>.
97. N. Ayedi, B. Rzig, N. Bellakhal, *Chem. Afr.* **2023**. <https://doi.org/10.1007/s42250-023-00628-0>.
98. H. A. Alharbi, B. H. Hameed, K. D. Alotaibi, S. S. Al-Oud, A. S. Al-Modaihsh, *Front. Environ. Sci.* **2022**, 10, 996953.
99. K. Jlassi, S. Mallick, A. Eribi, M. M. Chehimi, Z. Ahmad, F. Touati, I. Krupa, *Sens. Actuators B: Chem.* **2021**, 328, 129058.

**Disclaimer/Publisher's Note:** The statements, opinions and data contained in all publications are solely those of the individual author(s) and contributor(s) and not of MDPI and/or the editor(s). MDPI and/or the editor(s) disclaim responsibility for any injury to people or property resulting from any ideas, methods, instructions or products referred to in the content.